

UNCLASSIFIED

AD 273 723

*Reproduced
by the*

**ARMED SERVICES TECHNICAL INFORMATION AGENCY
ARLINGTON HALL STATION
ARLINGTON 12, VIRGINIA**



UNCLASSIFIED

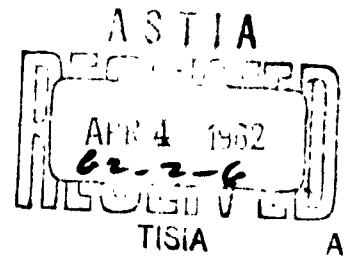
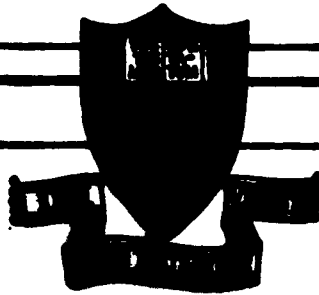
NOTICE: When government or other drawings, specifications or other data are used for any purpose other than in connection with a definitely related government procurement operation, the U. S. Government thereby incurs no responsibility, nor any obligation whatsoever; and the fact that the Government may have formulated, furnished, or in any way supplied the said drawings, specifications, or other data is not to be regarded by implication or otherwise as in any manner licensing the holder or any other person or corporation, or conveying any rights or permission to manufacture, use or sell any patented invention that may in any way be related thereto.

CATALOG BY ASTIA

273723

AS AD NO.

273 723



PRINCETON UNIVERSITY
PLASTICS LABORATORY

PLASTICS LABORATORY

TECHNICAL REPORT

No. 64A

**SYNTHESIS AND CHARACTERIZATION OF
SOME HIGHLY CONJUGATED SEMI-CONDUCTING**

POLYMERS

E.H. Engelhardt and H.A. Pohl

1 January 1962

**Contract No. DA-36-039sc-89143
NR 356-375**

**"Reproduction, translation, publication
use and disposal in whole or in part by or for
the United States Government is permitted".**

**The work reported here was supported
jointly by the Army, Navy and Air Force under
Signal Corps Contract DA-36-039sc-78105; DA
Project 3A99-15-001; ONR Project NR 356-375.**

**SYNTHESIS AND CHARACTERIZATION OF SOME
HIGHLY CONJUGATED SEMI-
CONDUCTING POLYMERS**

by

**H. A. Pohl and E. H. Engelhardt
Princeton University
Plastics Laboratory
Princeton, New Jersey**

ABSTRACT

A series of highly conjugated, semiconducting polymers was synthesized and electronically characterized. The conductivities of polymers, produced in this program, ranged from approximately 10^{-3} to 10^{-11} mho cm^{-1} at room temperature. A correlation between conductivity in PAQR polymers, and the size of the aromatic hydrocarbon monomer, was established.

Thermoelectric power measurements, and a Hall determination generally indicated p-type conductivity in the polymers.

Additional electrical determinations included:

Thermal activation energy of conduction, ohmic behavior, carrier species, electron spin density, thermal and chemical stability, and photo-electrical effects.

The electronic nature of conduction in the polyacene quinone radical polymers was proven by observing a large (positive) Hall coefficient, and by observing the stability of conduction to large charge passage.

Nonohmic behavior was observed at low electric field strengths.

SYNTHESIS AND CHARACTERIZATION OF SOME HIGHLY CONJUGATED SEMI-CONDUCTING POLYMERS

by

H. A. Pohl and E. H. Engelhardt

Semiconductors, as presently regarded, are materials which have electrical conductivity characteristics somewhere between those of insulators and metals. They are broadly characterized by a conductivity at room temperature in the range 10^3 mho/cm down to about 10^{-12} or 10^{-14} mho/cm. Additional criteria which are useful in differentiating semiconductors from metals may include a positive temperature-conductivity coefficient, a high sensitivity to certain impurities or to morphology, and, a high Seebeck or Hall coefficient.

In recent years the literature on organic semiconductors has increased considerably. Comprehensive reviews have been made by Akamatsu^{1,3}, Eley¹¹, Garrett¹⁶ and Pohl³⁸⁻⁴⁰. The organic semiconductors developed to date, all of which are based on a high degree of conjugation, may be conveniently considered almost without exception in two broad categories, (a) crystals of monomeric solids, or (b) polymeric bodies. The latter may be bonded datively (as in the donor-acceptor complexes), covalently (as in conventional organic polymers) or ionically (as in the salts of organic ions). The smaller organic monomers, such as naphthalene and anthracene are insulators^{1,45,50}. Some of the larger^{11,50} (e.g. violanthrone³ B or the phthalocyanines^{45,48}), show appreciable semiconduction.

The datively bonded charge transfer complexes may show considerable conduction^{1,2,11,19,20,21,24}, some as high as 10^{-1} mho/cm,

but they are generally of low thermal stability.

Polymers with extensive conjugation and highly enhanced electronic properties are formed, for example, by the destructive cyclization^{5,51,52} of organic materials. The heat-induced dehydrochlorination of polyvinyl chloride and polyvinylidene chloride copolymers, the dehydration of sugar⁴⁷, and the pyrolysis of many organic compounds at temperatures above 400° - 600°C are all examples of this technique.

Work in the field of pyrolyzed polymers and polymer carbons has been reported for example by Baker^{51,52}, Mrozowski^{30,31}, Oster³², Pohl^{23,34-40}, and Turkevich⁴⁷.

Directly synthesized semiconducting polymers, as opposed to pyrolytic polymers have only recently been reported.

In 1959, Pohl and Itoh^{6,40} prepared a large number of semiconducting phenolphthalein-type polymers, made by reacting various phenols with acid anhydrides. McNeill and Weiss^{27,28} reported on the preparation of xanthene-type polymers related to fluorescein. Conductivities as low as 1.4×10^{-4} mho/cm were observed.

A polymeric copper phthalocyanine with semiconducting properties has been prepared by replacing phthalic anhydride with pyromellitic dianhydride in the phthalocyanine dye synthesis^{13,14}. Eley reported¹² work on dehydrated proteins, which showed very low conductivities for the most part.

Berlin⁴ has recently written an excellent review of Russian work on highly conjugated polymers. Several directly synthesized semiconducting polymers including polyphenyleneazo-compounds and a polymer of diethynyl benzene were reported on.

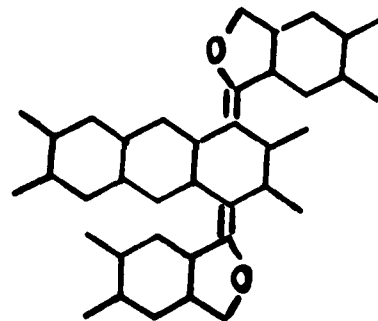
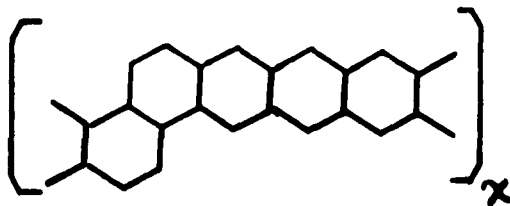
EXPERIMENTAL

It seems probable that a prerequisite for enhanced electronic behavior in organic polymer systems is that they contain a set of highly conjugated systems. Until recently, polymers which might meet this criterion have generally been purposefully avoided. This necessitated our development of new classes of polymers, only several of which had previously been described. The materials synthesized in this study include condensation polymers of acenes with aromatic acid anhydrides, condensation polymers of 1,2,4,5 tetra-bromobenzene; condensation polymers of di-isocyanates and quinones; and aniline black polymers. Studies were made using various useful physical parameters such as ESR, Seebeck coefficient (thermoelectric power), Hall effect, non-ohmic character, specific conductivity and its temperature coefficient, and the electronic (vis-a-vis ionic) nature of the conduction.

Synthesis

1. POLY ACENE QUINONE RADICAL POLYMERS (PAQR - Polymers).

The relative ease of synthesis, and the interesting electronic nature of the quinone and lactone structures, (incided) the investigation of a polymer class based on various acene nuclei, linked by both quinone and lactone groups.



A synthesis analogous to that commonly employed for making simple quinones was used to condense pyromellitic dianhydride with analogues of naphthalene.

The Freidel-Crafts type of reaction on an acid anhydride or acid chloride is one of the most useful methods for affecting inter and intra molecular acylations. A wide variety of conditions for acylations, using Lewis acids, are available from the literature⁸, 44,46,54.

In this study, two independent methods were used for condensing derivatives of pyromellitic acid, etc., with a number of acenes.

PAQR-I, Polymers - The first procedure involved reaction of pyromellitic dianhydride, and phthalic anhydride, with several aromatics, to produce a homologous series of polymers.

The desired molar ratio, of anhydride and acene, was mixed in a mortar. Generally 2 moles of zinc chloride catalyst were added per mole of acid anhydride. After thoroughly mixing the components, they were placed in a 150 x 20 mm. test tube and heated for the desired time, in a constant temperature bath. Since it was determined that the presence of air, during reaction, had very little effect on conductivity of the polymers, the reaction tubes were merely stoppered. The majority of polymerizations were carried out at 256 or 306°C, for 24 hours.

At the completion of polymerization, the polymers were ground to fine powders. The materials were leached with dilute hydrochloric acid for 12 hours, to aid in removing the zinc chloride catalyst. Subsequent to the leaching, the powders were extracted, with water

for 12 hours, ethanol for 24 hours and benzene for 12 hours, in a Soxhlet apparatus. The polymers were then dried at 50°C for 12 hours. After drying, the materials were again finely ground and stored in a desiccator until evaluations were to begin.

PAQR-II, Polymers - Polymers were also prepared by the Freidel & Crafts synthesis, employing AlCl_3 as a catalyst, and nitrobenzene as a solvent.

Pyromellitoyl chloride was prepared by gently refluxing pyromellitic anhydride with a large excess of thionyl chloride, in a 250 ml. round bottom flask, for approximately 48 hours. After this period, the excess thionyl chloride was vacuum distilled from the acid chloride, and 100 ml. nitrobenzene was added to the reactor. The contents were cooled in an ice bath. Anhydrous aluminum chloride was slowly added to the agitated mixture, until the molar ratio was slightly in excess of 4 catalyst to one pyromellitoyl chloride. After allowing enough time for complex formation between the AlCl_3 and nitrobenzene, as evidenced by solution of the catalyst, the hydrocarbon was slowly added to the cooled mixture, in equal molar quantity to the acyl chloride.

The reaction was generally quite exothermic, and adequate cooling was maintained until all of the acene had been added.

After completion of the acene addition, the solution viscosity generally increased rapidly and the exothermic reaction subsided.

The reactor was then warmed to approximately 50°C and agitation continued, until the viscosity became prohibitively high. After the agitation stopped, generally within 2 hours, the reaction mixture was allowed to stand at room temperature for 24 hours.

Unspent aluminum chloride was deactivated by slowly adding the contents of the reactor to cooled dilute hydrochloric acid.

The subsequent purification procedure was the same as that previously described for the zinc chloride catalyzed polymers.

2. POLYACENES.

An attempt was made at preparation of polyacenes, using a procedure similar to that previously outlined by Edwards and Goldfinger¹⁰. The reaction involved the condensation of 1,2,4,5, tetrabromobenzene by a Wurtz-Fittig type reaction.

A sodium-potassium alloy was prepared by adding 9.2 gm Na to 7.8 gm K, and refluxing the mixture, for 12 hours, under 20 ml of xylene. The alloy, a liquid at room temperature, was placed in a dropping funnel, and kept under xylene.

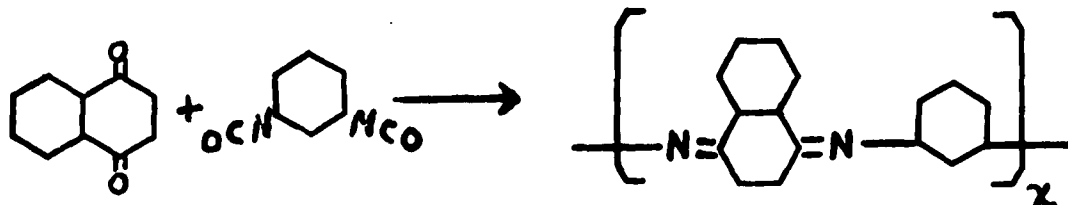
A 350 ml, 3 necked flask, provided with a reflux condenser and agitation, was used for the reaction. Recrystallized 1,2,4,5, tetrabromobenzene (39.4 gm) was dissolved in 50 ml of dioxane, and the mixture was heated to 95°C.

The dropping funnel was placed on the reactor. After turning off the heater, alloy was slowly added to the mixture (for approximately 3 hours). After the reaction subsided, external heating was applied and the reaction continued at a temperature of 95°C for approximately 36 hours.

The yellow-red, polymeric material was separated from the solvents and washed with ethanol to safely remove all traces of the metals. After washing with hexane, and drying, the polymer was ground, and extracted with water, ethanol and benzene. The fractions soluble in hot ethanol and benzene were recovered by evaporation.

3. QUINAZONE POLYMERS.

Another material with potentially highly conjugated structure was made by reacting di and tri isocyanates with quinones. The reaction, which was reported by Lieser and Nischk²⁵;s;



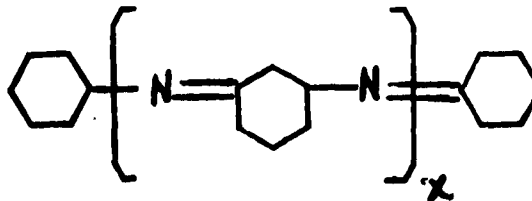
Polymerizations were attempted by heating equimolar quantities of quinones and poly functional isocyanates, in the absence of air, to temperatures as high as 300°C. A reaction was immediately apparent from formation of a deep brown color. Depending on temperature, the mass remained liquid for a certain period of time and then rapidly solidified. Deep brown, insoluble, infusible materials were produced. The polymers were ground and extracted in the manner previously described for the polyacene quinones.

4. ANILINE BLACK POLYMER.

A number of references in the literature describe resistivity measurements on various commercial aniline dyes^{7,48}. In our studies, we synthesized a polymeric material from pure aniline, primarily for comparative purposes.

Distilled aniline was reacted with dilute hydrochloric acid to form the aniline hydrochloride. Sodium chlorate was added to the aqueous solution, and dissolved. After solution was complete, the mixture was gently heated, with good agitation. Within several minutes, an exothermic reaction occurred, and a black precipitate formed. This material, which is soluble in ethyl-ether, was thoroughly extracted with water and ethanol. A suggested structure for

this polymer was given by Packer³³ as:



C. EVALUATION PROCEDURES

1. PREPARATION OF MATERIALS FOR ELECTRICAL MEASUREMENTS.

Generally all of the polymers evaluated in this program were insoluble, infusible materials, and were consequently powdered and examined as compacted pellets.

2. RESISTIVITY MEASUREMENTS.

Resistivity of the polymers was measured by a DC technique, using field strengths below 150 volts per centimeter.

The powdered polymers were contained in a steel cell, with platinum contacts, capable of being loaded to pressures in excess of 10,000 kg/cm². Tetrafluoroethylene and Nylatron (nylon polymer containing ca. 30 percent MoS₂) were used as electrical insulators.

An inherent cell resistance well in excess of 10¹⁵ ohms was determined by measurements with mica spacers. This cell limitation was several orders of magnitude higher than the maximum values of interest in this study.

The sample temperature was measured by placing a copper-constantan thermocouple in close proximity. Electrically heated aluminum platens were employed for temperature variations.

In order to compact the powders uniformly, for comparative purposes, the cell and platens were placed in a Preco press, and

a standard load was applied. Two, 2-inch phenolic blocks insulated the cell assembly from the press. The resistance cell, and circuitry, are depicted in Figures 1 and 2.

Several techniques were employed for measuring the sample resistance, depending on the range involved. Resistances below 10 ohms were measured in a Wheatstone bridge circuit. A Triplet, model 630 NA, ohm meter was used for measurements between 10^1 and 10^5 ohms. A precision of ± 2 percent was obtained. Resistances in excess of 10^5 ohms were measured with a General Radio Corp., type 544-B, Megohm bridge. Precisions of ± 5 percent were obtained.

As has been previously mentioned, the polymer resistivity samples were in the form of fine powders, which were stored in a desiccator over silica gel. Prior to measurement, the resistivity samples were carefully weighed on an analytical balance in order to facilitate apparent density determinations at the applied load.

The routine, for room-temperature resistivity measurements, consisted essentially of placing the powdered sample in the cell, placing the apparatus in the press, slowly applying the desired load and connecting the proper meter. Triplicate determinations were made for each sample.

The temperature-resistivity relationships were determined in an essentially similar manner. The sample temperature was adjusted by presetting the current to the platen heaters, and allowing the system to achieve thermal equilibrium at the specific heat input rate. Five uniformly staggered measurements were made between limits of approximately 25°C and 100°C. Determinations were made at descending temperatures, and repeated under ascending conditions. Measurements were taken only after the temperature equilibrium of the sample was ascertained.

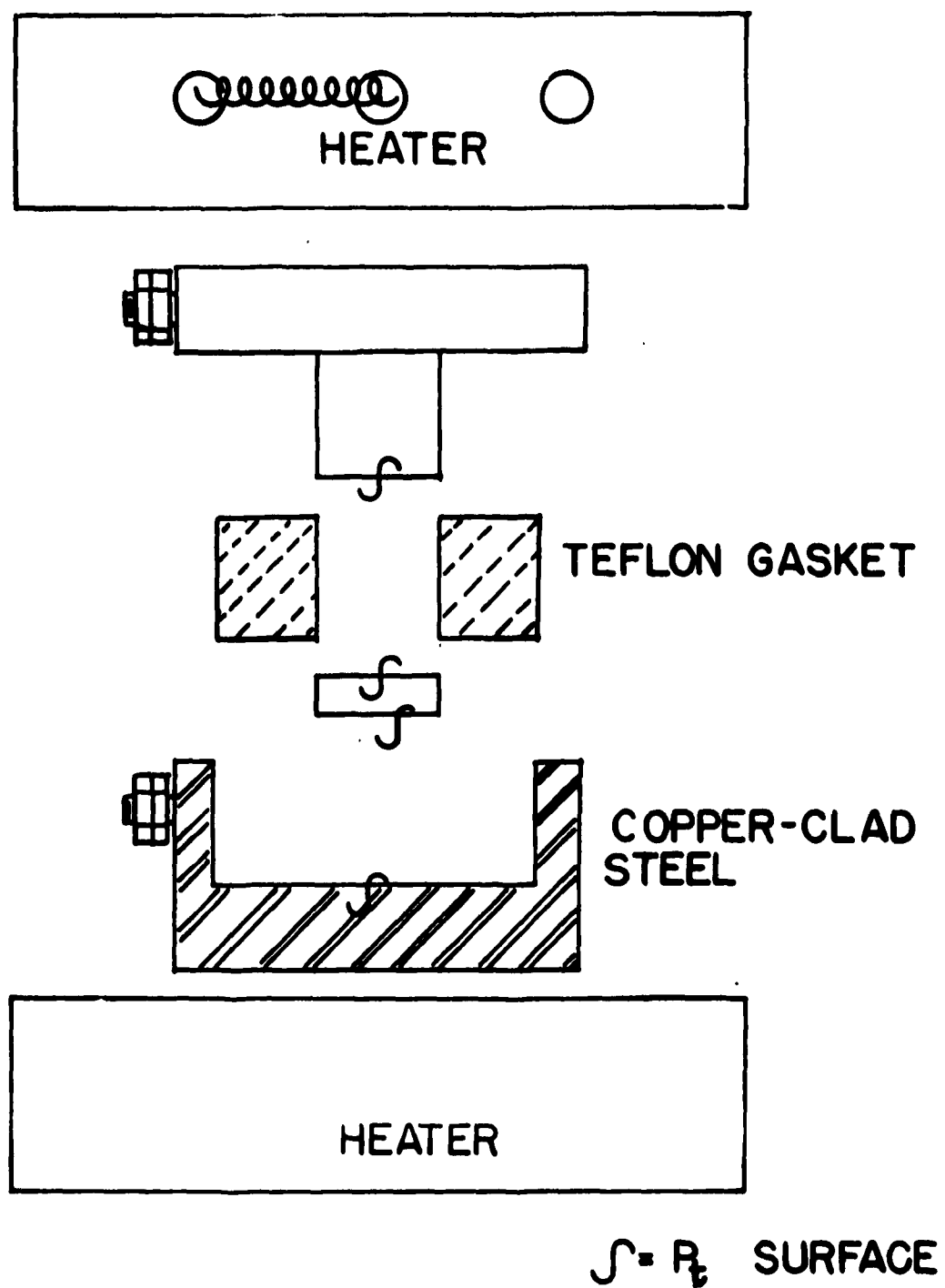
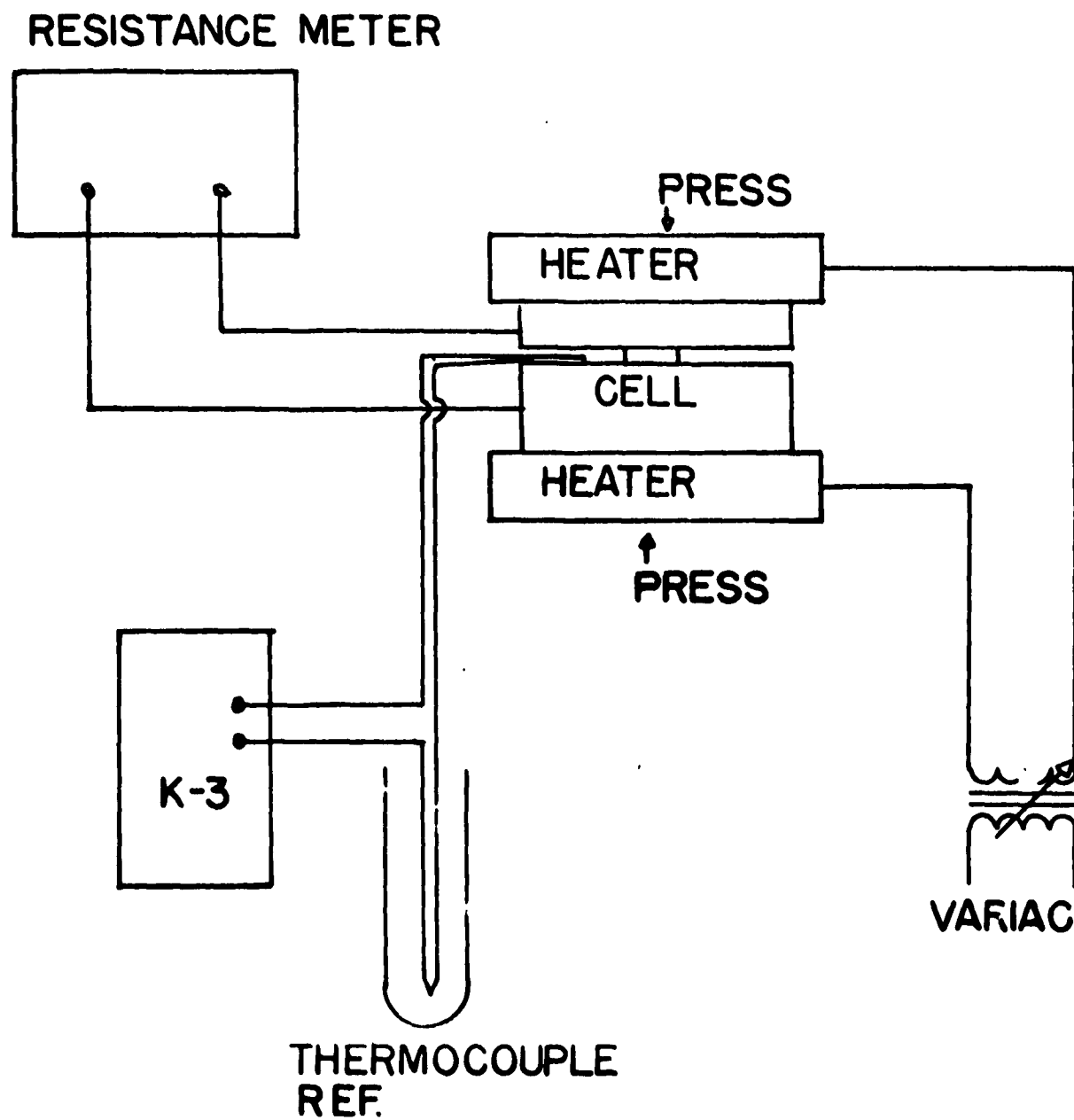


Figure 1, Resistivity Cell.



**Figure 2, Electrical Circuit For Resistivity And
Activation Energy Measurements.**

After completion of each electrical measurement, the sample thickness was measured, and recorded. The compacted pellets were 0.96 cm. in diameter and approximately 0.1 cm. thick.

3. THERMOELECTRIC POWER.

The Seebeck coefficient, and related parameters, of several polymers, were studied as a function of average sample temperature, temperature gradient across the sample, and compaction pressure.

A cylindrical cell, with a sample contact surface area of approximately 4.3 cm^2 was constructed for the measurements (Figure 3). The basic blocks were machined from aluminum in order to minimize thermal gradients between the sample and points of temperature measurement.

A floating sample retainer, made from tetrafluoroethylene, was provided to maintain a uniform distribution of the powdered sample under load, and in addition, to minimize the temperature gradient across the contact surfaces. The actual sample contacts were platinum foil^s spotwelded to platinum wire. Copper-constantan thermocouples were placed in small, milled grooves at the aluminum platinum interfaces. An aluminum filled epoxy was employed to improve thermal contact between thermocouple, aluminum heat sink and platinum foil. In order to minimize anomolous values, due to stray currents, the thermocouple circuit was completely disconnected (by a gang switch) while thermal voltage was being measured, and vice-versa. The platinum wires were connected to copper leads through a duel mercury junction, insulated to assure that both platinum-mercury-copper junctions were at the same temperature.

Both thermal EMF, and the sample temperature, gradient, were measured with a Leeds-Northrup, K-3 potentiometer. All circuitry was guarded by grounded shielding, in order to minimize stray EMFs.

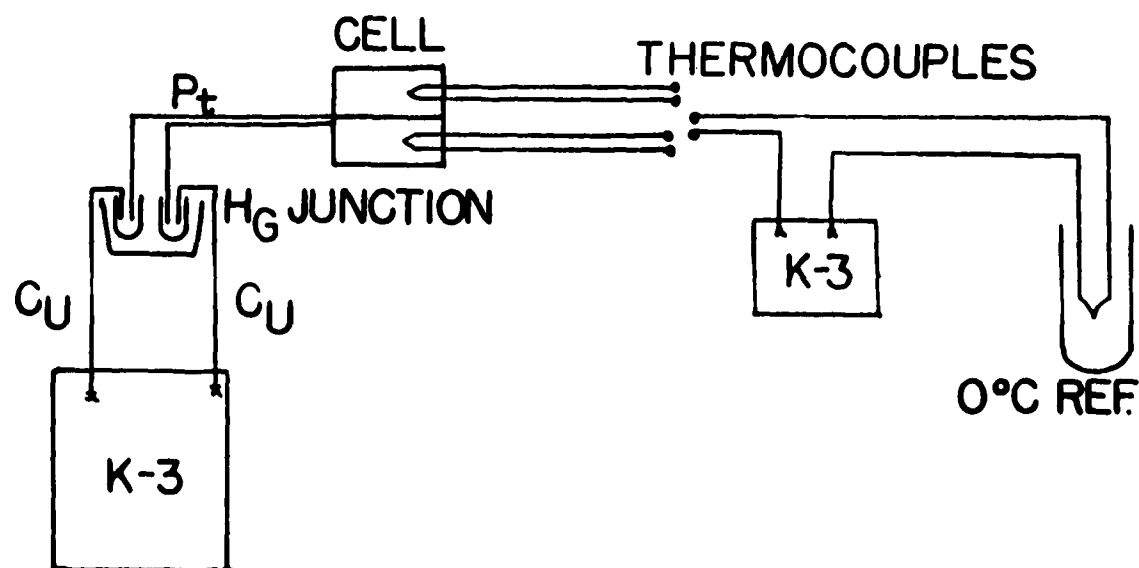
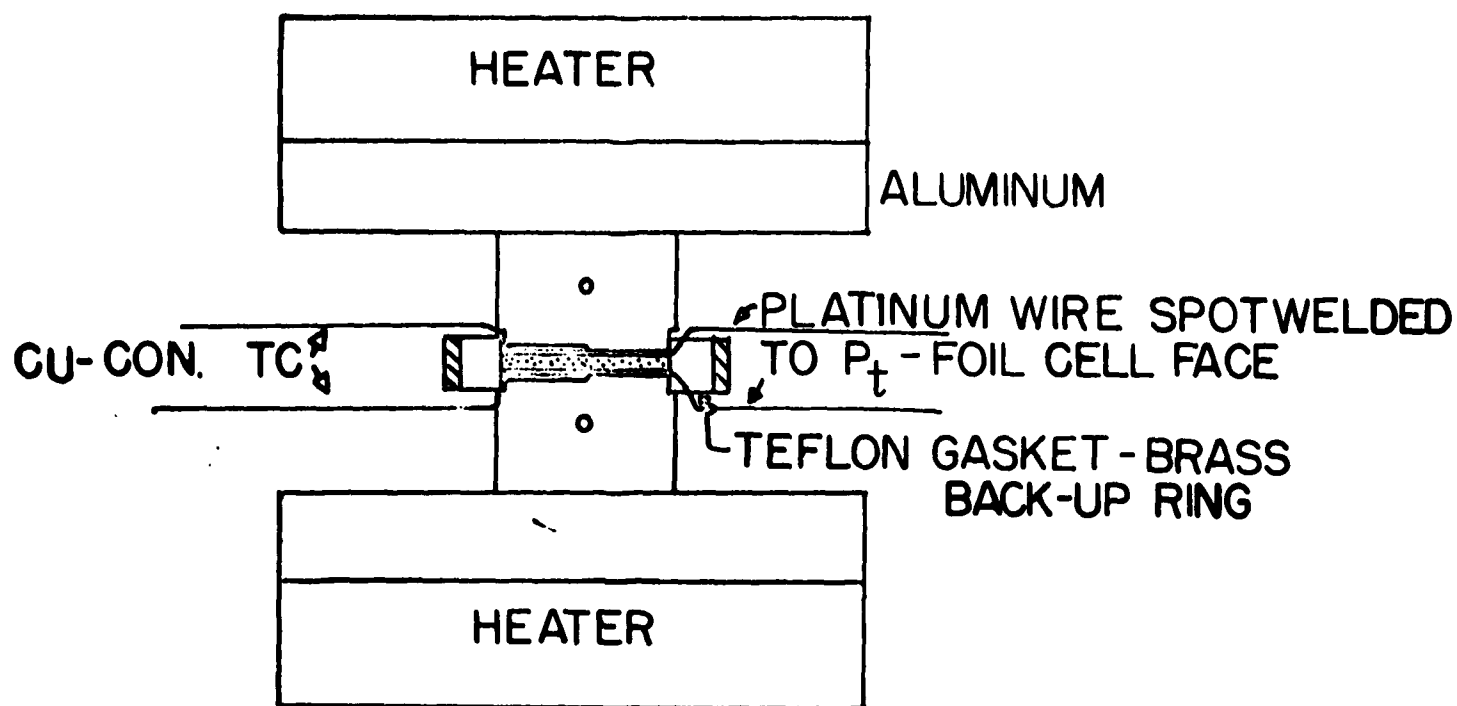


Figure 3, Apparatus And Electrical Circuit
For Measuring Seebeck Coefficient.

The desired average sample temperature was maintained by using the aluminum heating platens previously described with the resistivity apparatus.

A 25 watt soldering pencil, connected to a Variac, was employed as a heater for establishing a temperature gradient across the sample. The heater was inserted in one of the aluminum blocks.

Measurements were made in a temperature range of approximately 25°C to 100°C, with temperature gradients of approximately 2, 5, 10 and 15°C for each sample.

As with the resistivity determinations, the system was allowed to approach equilibrium closely before making measurements.

The thermoelectric apparatus was insulated from the platens of the Preco press by 2-inch phenolic slabs.

In order to minimize error, due to the inability to make all readings simultaneously, the temperatures were measured at equal time intervals, before and after measurement of Seebeck voltage. An average of these readings was employed in calculating the temperature gradient values.

The Seebeck coefficient, was calculated by use of the relationship:

$$Q = \frac{\Delta V}{\Delta T} = \mu V / ^\circ C, \text{ microvolts per degree C.}$$

where ΔV is the thermal EMF across the platinum-polymer-platinum junctions, and ΔT the thermal gradient between platinum electrodes.

Values of thermoelectric power presented in this paper have been corrected for the effect of platinum, and are therefore absolute. Values for the absolute thermoelectric power of platinum were obtained from the work of Wilson⁵³.

4. HALL COEFFICIENT.

A 2000 turn electromagnet was used to provide a magnetic field of approximately 17K Gauss, for Hall voltage determinations.

Polymer samples were compacted into briquettes, 1 inch by 1/4 inch, by 1/16 inch, and placed into a special yoke for proper insertion between the magnet poles. The yoke, shown in Figure 4 contained the customary end contacts for carrier supply, as well as the Hall contacts for measuring transverse potential gradient.

The transverse potential gradient of samples in a magnetic field was measured with a Leeds-Northrup Model K-3 potentiometer. Magnetic field strength, and direction, as well as current through the sample were recorded. A diagram of the Hall apparatus is presented in Figure 5.

The transverse EMF gradient, induced by the magnetic field, was obtained by reversing the field several times and recording the potential with each field direction. Average values for each field direction were then used to obtain the Hall voltage.

$$EMF = \frac{(A + \Delta EMF) - (A - \Delta EMF)}{2}$$

where A = Asymmetric potential of the sample

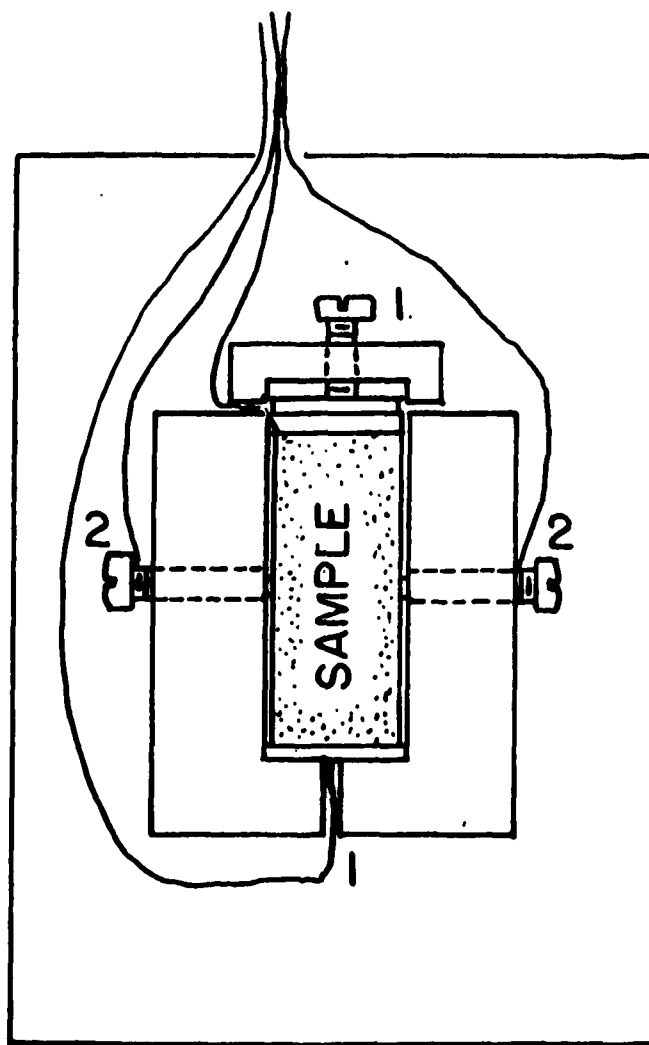
ΔEMF = Hall voltage

The Hall coefficient, (R_H), was then calculated by the following relationship:

$$R_H = \frac{t \cdot V \cdot 10^8}{I \cdot H}$$

where

I = longitudinal current (amps)
 H = field strength (Gauss)
 t = thickness of sample (cm)
 V = Hall Voltage (Volts)
 R_H = Hall coefficient (cm³/coul)



1. CARRIER CONTACTS
2. HALL VOLTAGE PROBES

Figure 4, Cell For Hall Coefficient Measurement.

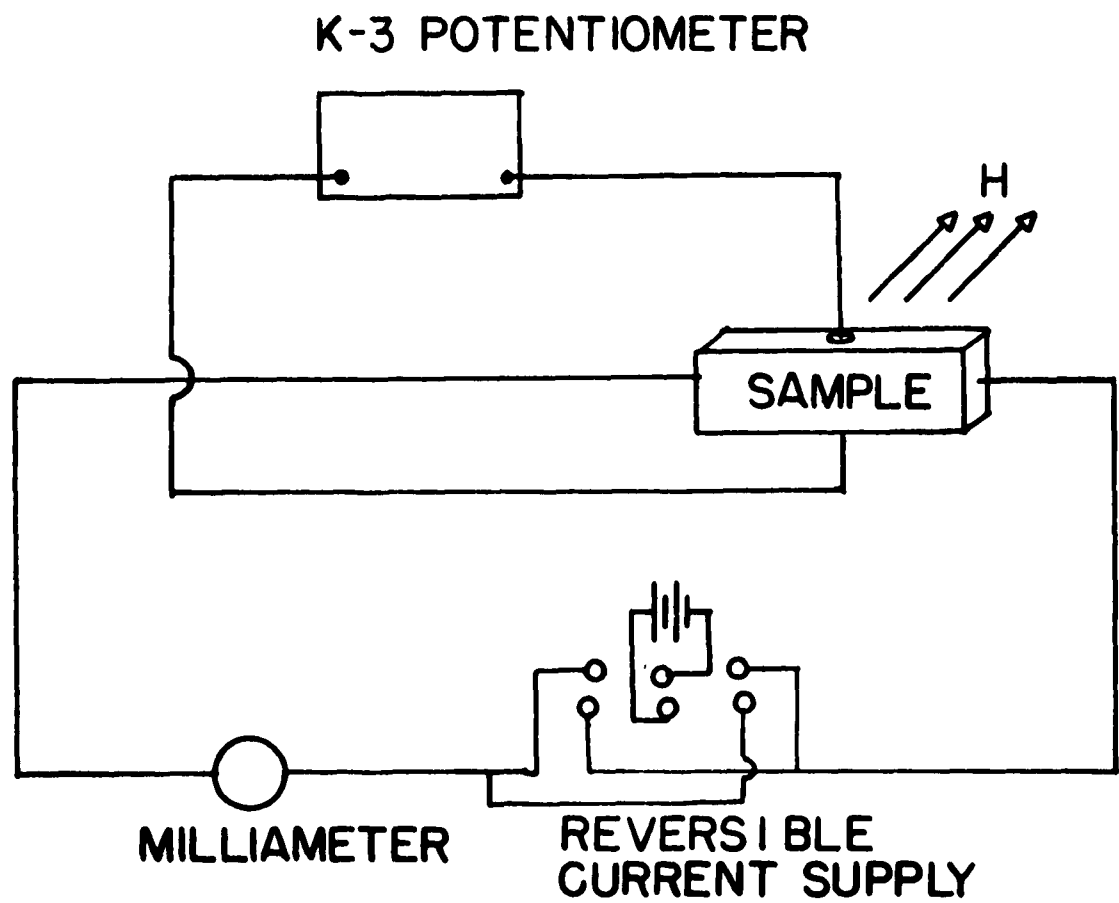


Figure 5, Electrical Circuit For Hall Coefficient Measurement.

5. ELECTRON SPIN RESONANCE.

The concentration of unpaired electrons in polymer samples, was determined by the electron spin resonance method. Spin concentrations in a number of polymers were measured in the equipment of Dr. R. Pressley, with his considerable assistance, at the Palmer Physical laboratory.

A carefully purified, (by ether crystallization), sample of di phenyl picryl hydrazil (DPPH) was employed as a standard. Polymer samples, in capillary tubes, were irradiated at a fixed frequency of 9550 megacycles. The magnetic field was slowly varied around a mean of approximately 15.2 K Gauss.

The unpaired spin concentration, in polymer samples, was obtained by direct comparison with the standard. Calculations involved in the determination, are presented in Appendix (I).

6. STRUCTURE ANALYSIS OF POLYMERS.

The generally insoluble, infusible nature of the polymeric products, synthesized in this program, severely hampered attempts to determine the structure. All attempts at infra-red and x-ray analyses of pressed pellets and Nujol mulls, were unsuccessful.

Chemical composition of the polymers was determined by submitting samples to Galbraith Laboratories for C, O, H and N analyses.

The level of residual zinc catalyst in the polymers was determined by irradiation of the sample, and measurement of zinc isotope decay. Dr. D. A. Ross and Mr. R. F. Bailey, at Industrial Reactor Laboratories, irradiated the samples and supplied the analytical information.

7. HEAT AND CHEMICAL STABILITY.

In an attempt to gain some insight as^{to} the conduction mechanism, several thermal and chemical post treatments were carried out on PAQR polymers.

Studies on the effect of temperature were carried out by placing polymer samples in 2 oz. glass ampules, and heating these to the desired temperature. Where thermal treatment under vacuum was desired, the ampules were evacuated and sealed before heating.

Chemical reactions were carried out in small test tubes, heated in constant temperature baths.

8. MISCELLANEOUS ELECTRICAL CHARACTERISTICS.

a. Non-ohmic character - The relationship between resistance and applied potential across a polymer, was measured by comparison of the sample with metal resistor which is Ohmic. The apparatus, essentially a Wheatstone bridge, is shown in Figure 6. The potential across the bridge was varied from 1.5 to 52 volts. Resistors R_1 and R_2 were set at 2000 ohms. The resistance of the polymer (R_x) was then necessarily equal to R_3 , at equilibrium.

b. Current carrier classification - The mode of conduction was determined by passing a D.C. current through a sample of polymer contained in the resistivity cell. An average current of approximately 0.3 amperes, corresponding to a potential of 75 volts, was applied for a period of several days. Current and resistance of the sample were measured periodically. In order to compensate for extraneous variables such as compaction pressure and room temperature fluctuations over the duration of the test, a control example, in an identical cell was employed. Results were obtained on the basis of resistance ratio of the material under test and the control.

OHMICITY APPARATUS

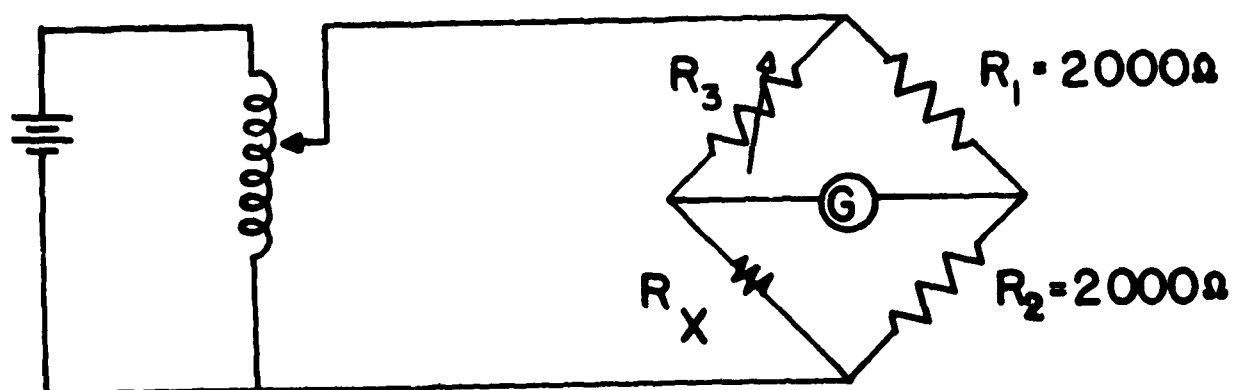


Figure 6, Apparatus For the Determination of Resistance
As A Function of Applied Potential.
 R_1 , R_2 , R_3 Are Wire Resistors.

9. PHOTO-CONDUCTIVITY.

A cursory look at photo-conductivity in PAQR polymers was made, using a relatively crude apparatus. A 500-watt projector, with a heat filter, was employed as the illumination source. The cell, and circuit, employed in the studies are shown in Figure 7.

Measurements of photo EMF were made, using a Keithley Model 150A Microvoltammeter, and a recorder. Photo-voltaic and photo-conduction effects were measured.

For the photo-conduction measurements, a standard EMF was placed across the sample, and current variations were recorded.

DISCUSSION OF RESULTS

A. GENERAL

Room temperature resistivities were obtained for all of the materials synthesized in this study. A range of approximately 10^2 to 10^{12} ohm cm was obtained. Except where specifically indicated, the compaction pressure for resistivity measurements was approximately 1800 ± 70 Kg/cm².

A comprehensive investigation of other electrical characteristics was carried out on several polymers representative of the entire range of room temperature resistivities.

B. PRESSURE - RESISTIVITY

In order to select an appropriate sample-compaction pressure for the bulk of the resistivity determinations, in this report, the relationship between resistivity and pressure was studied for three representative polymers. Results are shown in Figures 8 and 9.

Below approximately 1000 Kg/cm², large incremental changes in resistivity were observed, probably due to the presence of voids

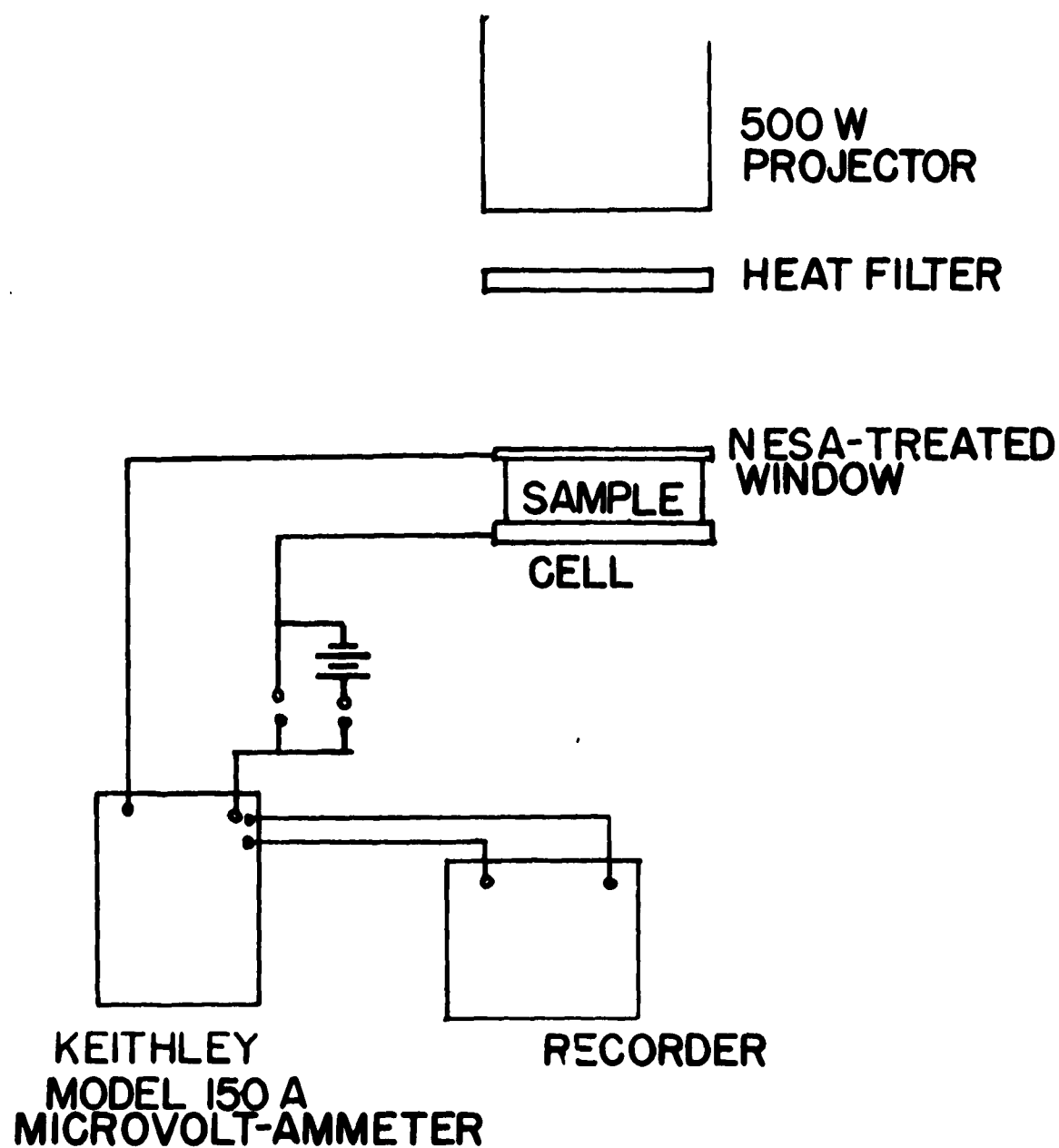


Figure 7, Circuit For The Measurement Of Photoelectric Properties.

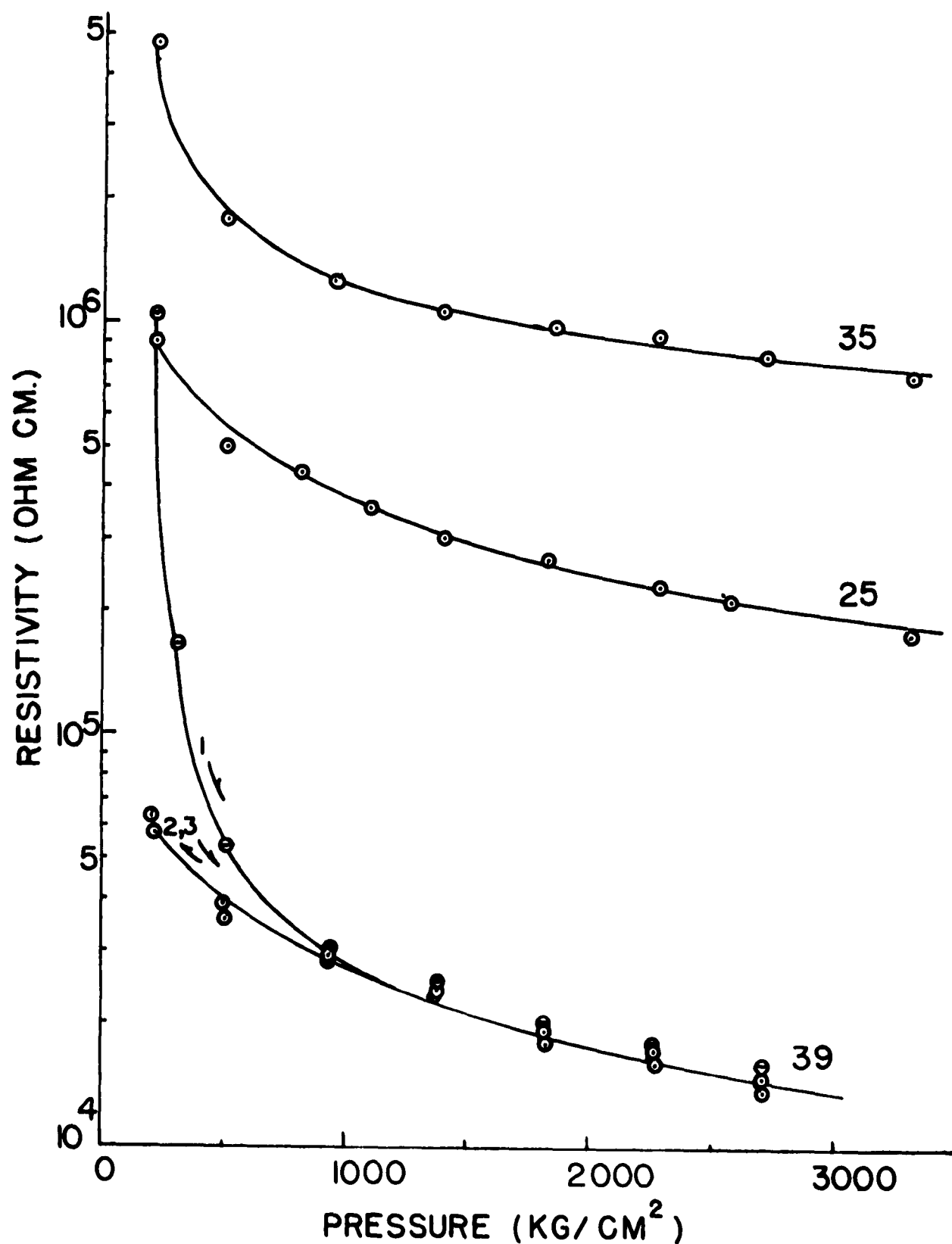


Figure 8, Effect Of Measurement Pressure On The Resistivity
Of PAQR Polymers. Curve Numbers Correspond
To Polymers Described In Tables 5&6.

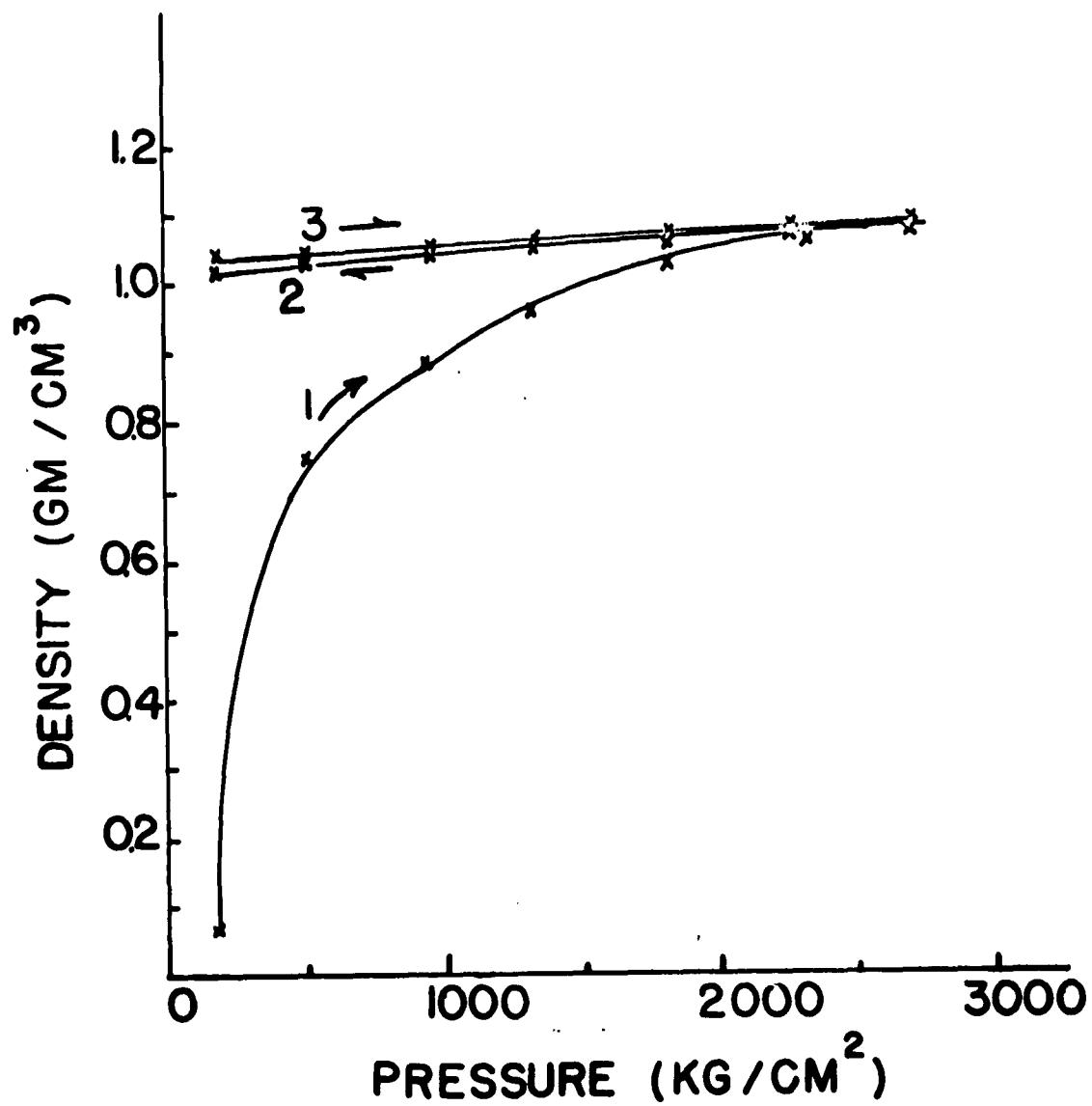


Figure 9, Effect Of Measurement Pressure On The Density Of PAQR Polymers. Curve #1, Taken On Initial Compression; Curves 2 And 3 Followed.

in the sample. At higher pressures, the elimination of voids probably becomes subordinate to the normal decrease in resistivity due to orbital overlap, etc.

Curve C shows the effect of repeated pressure cycling on the resistivity-pressure characteristics. After one compaction cycle above 1500 Kg/cm², the materials exhibit essentially reversible behavior.

Based on the observed characteristics, a compaction pressure in excess of 1500 Kg/cm² was deemed necessary to insure reliability of measurements. In order to conveniently compare the results of this investigation with concurrent work^{6,41,42}, in this laboratory, on other directly synthesized semiconductors, a compaction pressure of 1800 \pm 70 Kg/cm² was used for the bulk of the resistivity determinations.

C. ZINC CATALYZED ACENE - QUINONE POLYMERS

1. POLYMERIZATION VARIABLES.

Reproducibility of Results - Three polymers, synthesized under similar conditions, were compared in order to obtain a cursory idea as to reproducibility. The results are outlined in Table I. An approximate batch-to-batch variability of approximately \pm 10 percent is indicated. Precision of resistivity measurements was estimated at roughly \pm 8 percent.

Polymerization Atmosphere - The effect of polymerization atmosphere on polymer properties was determined by comparing resistivities of polymers made in air and under a nitrogen blanket. Results, which are summarized in Table II, indicate that the presence of oxygen during the synthesis increases polymer resistivity. The effect, however, was rather small, considering the overall

TABLE I

Reproducibility of Results

Polymerization Conditions*			
<u>Temperature (°C)</u>	<u>Time (hr)</u>	<u>Resistivity (ohm cm)</u>	<u>Density (gm/cc)</u>
306	24	2.33×10^5	1.20
306	24	2.35×10^5	1.24
306	24	2.67×10^5	1.27

TABLE II

Effect of Polymerization Atmosphere

Polymerization Conditions*				
<u>Temperature (°C)</u>	<u>Time(hr)</u>	<u>Atmosphere</u>	(ohm cm) <u>Resistivity</u>	<u>Yield (%)</u>
306	24	Air	2.72×10^5	15.5
306	24	Nitrogen	1.14×10^5	14.5
306	24	Nitrogen	9.05×10^4	18.2

* (1:1:1, PMA : $Z_n Cl_2$: Phenanthrene)

variations experienced in this study.

- Time and Temperature of Reaction - The effect of polymerization time and temperature was studied on two zinc catalyzed PAQR polymers. Resistivities, as a function of polymerization conditions, for a pyrene PAQR polymer, and a phenanthrene PAQR polymer, are shown in Figures 10 and 11.

In general, resistivity of the PAQR polymers decreased with increasing polymerization temperature.

The relationship between resistivity and time, at constant temperature, was found to differ somewhat for the two polymer systems; however, after approximately 24 hours of reaction, all samples behaved similarly. Subsequent to 24 hours reaction, the resistivity of PAQR polymers generally decreased slightly with polymerization time.

Formation of extensive conjugated systems was evidenced by the color changes during polymerization. Product color changed from white to yellow to orange to deep red and finally black. The degree of polymerization and extent of conjugation were generally high enough to effect the black appearance within two hours.

Optimum polymerization conditions, as determined by resistivity of the samples and yield, were approximately 250-300°C, for 24 hours.

Temperatures below 200°C were inadequate for polymerization with the zinc chloride catalyst. Very low yields of polymer, having relatively high resistivity, were obtained at 200°C.

High material losses were encountered when polymerizations

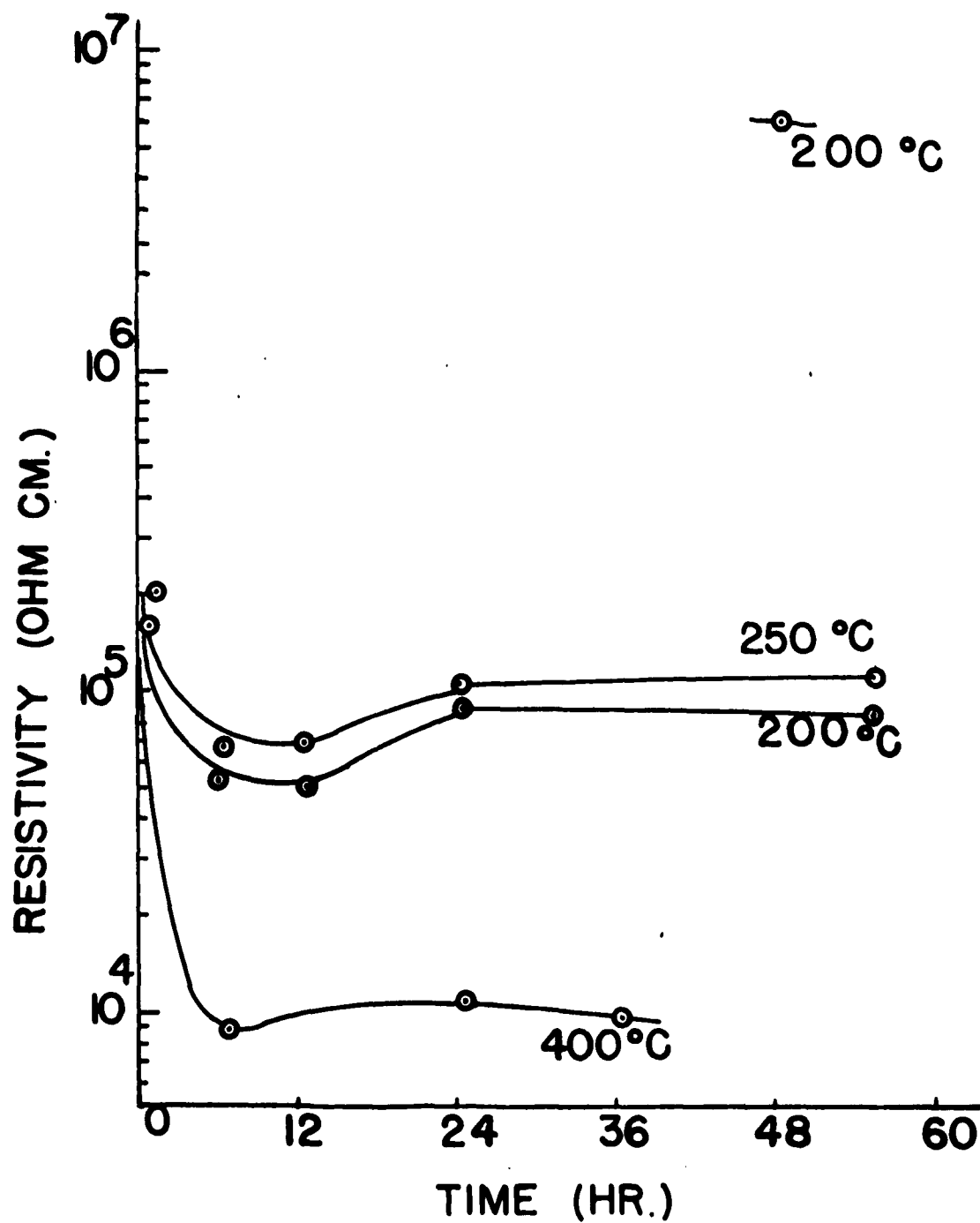
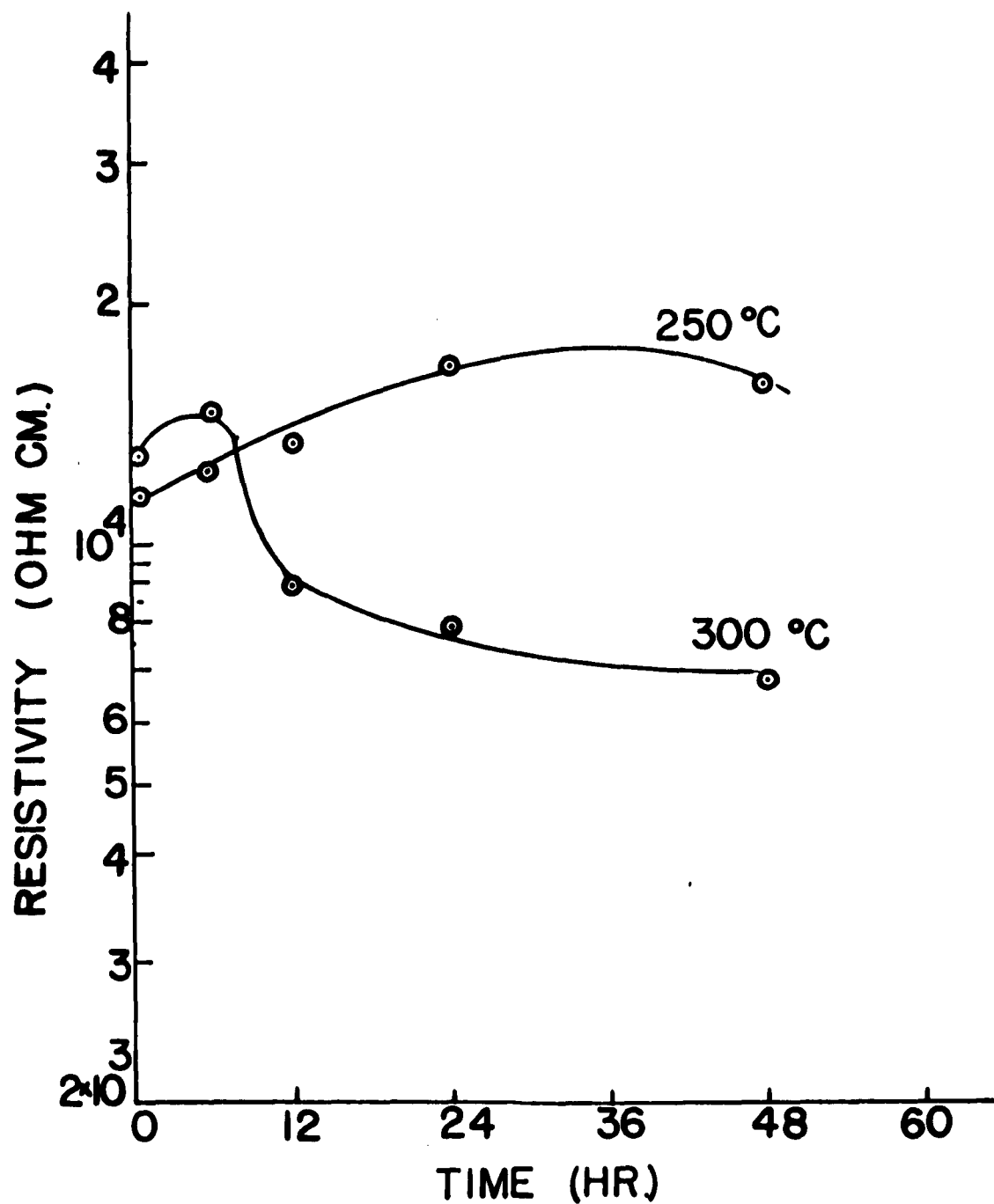


Figure 10, Effect Of Synthesis Time And Temperature

On The Resistivity Of A PAQR Polymer.

The Polymer Composition Is 1:1:1, Phenanthrene
: Pyromellitic Dianhydride : ZnCl₂.



**Figure 11, Effect Of Synthesis Time And Temperature
On The Resistivity Of A PAQR Polymer.
The Polymer Composition Is 1:1:1, Pyrene
: Pyromellitic Dianhydride : ZnCl_2 .**

were run at temperatures much in excess of 300°C.

Catalyst Concentration - The effect of the ratio of zinc chloride (catalyst) to pyromellitic dianhydride, was studied on a phenanthrene PAQR polymer. The ratio of phenanthrene to pyromellitic dianhydride was maintained 1:1.

Resistivity of polymers was found to decrease with increasing catalyst concentration. The results, shown in Table III also show that polymer yield was markedly improved with increasing catalyst concentration. It was noted, in addition, that the amount of ethanol-soluble organic material decreased markedly with increasing zinc chloride concentration. This indicated that increased catalyst concentrations led to higher degrees of polymerization.

No insoluble polymer was formed when pyromellitic dianhydride or acenes were heated either separately or combined, in the absence of zinc chloride. Zinc chloride did not catalyze condensations of the separate monomers to insoluble polymers. It was therefore concluded that all three components were necessary for polymerization.

The residual zinc contents of several PAQR polymers, as determined by radio zinc isotope decay, are summarized in Table IV. No relationship between polymerization conditions and residual catalyst was apparent.

2. POLYMER COMPOSITION AND STRUCTURE

The zinc chloride-catalyzed PAQR polymers were, in all cases black, insoluble, infusible materials. Yields expressed as the ratio of polymer-to-dianhydride plus acene, ranged from approxi-

TABLE III

Effect of Catalyst Concentration

Polymerization Conditions*

<u>mole Zn Cl₂/mole PMA</u>	<u>Temperature (°C)</u>	<u>Time (hr)</u>	<u>Resistivity (ohm cm.)</u>	<u>Yield %</u>
0.5 / 1	306	24	2.3×10^5	15.5
1 / 1	306	24	1.9×10^5	13.6
3 / 1	306	24	1.3×10^5	35.4
no catalyst	306	24	-	0

TABLE IV

Analysis of Residual Zinc Content in Typical
Acene Quinone Radical Polymers

<u>Sample Designation</u>	<u>Polymer Description</u>	<u>Zinc Content (PPM)</u>
35	1 mole anthracene/1 mole PMA	1.4
38	1 mole phenanthrene/3 moles PMA	4.0
39	1 mole pyrene/1 mole PMA	1.9
41	1 mole chrysene/1 mole PMA	5.3
42	1 mole chrysene/3 moles PMA	1.8

* 1 mole phenanthrene per mole PMA

mately five percent to fifty percent, depending on the reactivity of the hydrocarbons.

Examination of the polymer structure by infra-red and x-ray analyses were unsuccessful, necessitating conclusions based on elemental analysis, and analogy with model syntheses reported in the literature.

Two general possibilities for reaction mechanism during acylation are encountered. One mechanism leads to the formation of a keto, or a quinone linkage; the alternate produces a lactone structure.

Several workers, including Marschalk²⁹, have published papers concerning the synthesis of quinones under conditions roughly similar to those employed in this study. Marschalk reported synthesis and positive identification of linear quinones, up to 11 rings, from reaction of pyromellitic dianhydride and naphthalene at 200°C.

The formation of lactones is also known to occur under the conditions employed in our zinc chloride-catalyzed system. A review of the literature indicates that this reaction seems to be predominant only when electron donating substituents are present on the acene. Such examples are based only on observations with benzene and its derivatives. The higher resonance stability of the larger acenes might well influence the ratio of quinone formation to lactone formation.

On the basis of analogy to past investigations, it was therefore inferred that a majority of the linkages would be keto

or quinone, as opposed to lactone. In addition to the directly formed links, a number of secondary linkages and groupings could have been formed. At the reaction conditions employed, semi-quinones, hydroquinones, etc. could have resulted from a partial reduction, rearrangement, acylation and other reactions of quinone groups, giving rise to a number of coexistent structures, many of which are known to be free radical⁴⁹.

Carbon, hydrogen, oxygen analyses for several polymers, made with equimolar quantities of acene and dianhydride, indicate that the polymers contain approximately 2 moles of acene per mole of pyromellitic dianhydride, with a loss of 2 moles of water:

<u>Sample 26</u>	C	O	H	
actual	64.2	4.6	31.2	(average of duplicates)
theoretical (assumes				
2 acene per PMA)	63.3	6.67	30.0	

<u>Sample 39</u>				
actual	63.4	6.0	30.6	(average of duplicates)
theoretical (assumes				
2 acene per PMA)	65.6	6.25	28.1	

Polymers made with a higher ratio of dianhydride, to monomer contained an increased percentage of oxygen.

Further discussion of polymer structure, and its relation to the semiconduction in the PAQR series, will be deferred until additional data have been presented.

Effect of Monomer - In an attempt to gain some insight as to the conduction mechanism in PAQR polymers, an "homologous" series was prepared. Fourteen aromatic nuclei were incorporated into the

zinc chloride-catalyzed pyromellitic dianhydride-acene polymer. The results are summarized in Table V. A definite decrease in resistivity was experienced as the size of fused aromatic nuclear portion of the acene component of the polymer increased. The correlation between acene size and polymer resistivity is presented in Figure 12. Information on the resonance energies of fused aromatics was too sparse to permit a correlation on this, perhaps preferable basis.

Monomer Ratio - The monomer ratio of acene-to-pyromellitic dianhydride, was found to influence the conductivity level of PAQR polymers. Higher percentages of acid dianhydride in the mixture of monomers, generally produced polymers of increasing resistivity. Results from the comparison of 12 polymer systems are summarized in Table VI.

A comparison of carbon, hydrogen, oxygen analyses, on polymers 39 and 40, shows that an increase in the percentage of acid dianhydride in the monomer resulted in a corresponding increase in the polymer. The C,O,H, analysis is presented in the following table:

Sample No.

	Moles PMA	Moles Pyrene	% C	% O	% H
39	1	1	83.90	10.57	3.33
40	3	1	77.24	15.30	2.72

Acid Anhydride - Polymers, formed by the condensation of acenes with phthalic anhydride, generally exhibited somewhat higher resistivities than the acene-pyromellitic dianhydride series. The results, of condensations with six aromatic hydro-carbons, are presented in Table VII.

TABLE V

Effect of the aromatic co-monomer on the room temperature resistivity of PAQR polymers.

<u>Sample No.</u>	<u>Acene</u>	<u>Polymerization Temperature</u>	
		<u>253°C</u>	<u>308°C</u>
, 50	Biphenyl		3.4×10^{10}
31, 51	Terphenyl	5.6×10^{10}	1.4×10^7
33, 52	Naphthalene	9.7×10^6	1.4×10^6
35, 53	Anthracene	8.3×10^5	3.2×10^5
37, 54	Phenanthrene	1.0×10^5	9.2×10^4
39, 55	Pyrene	1.6×10^4	7.6×10^3
41, 56	Chrysene	1.6×10^5	2.1×10^4
46, 58	Tri phenylchloromethane	4.6×10^{11}	3.7×10^9
66, 67	Tri phenyl methane	5.8×10^{11}	3.1×10^9
48, 59	Fluoranthrene	4.4×10^5	3.5×10^5
, 85	Perylene		1.8×10^5
, 86	Dibenzpyrene		9.5×10^2
, 87	Picene		1.6×10^4
68,	Ferrocene	1.7×10^9	

Note: ACENE/PMA/Zn Cl₂ = 1/1/2

Polymerization time = 24 hr.

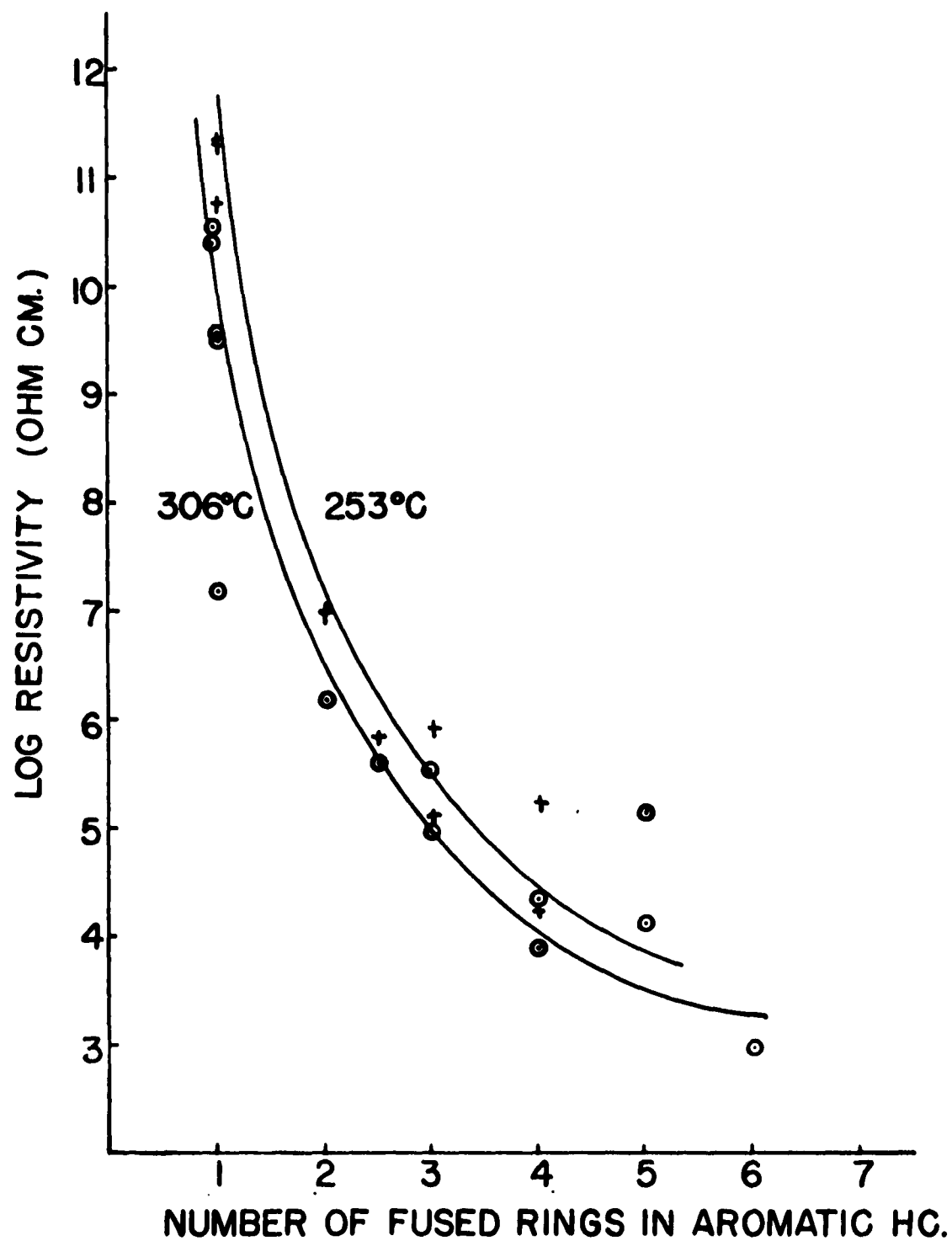


Figure 12, The Effect Of Acene Size On The Resistivity_{25C} Of PAQR Polymers.

+ = Polymerization At 253C

⊙ = Polymerization At 306C

TABLE VI

Resistance of FAQR Polymers as a
Function of Monomer Ratio

SAMPLE DESIGNATIONS	POLYMER TYPE	RESISTIVITY (Ωcm) at 25°C			
		1 mole Hydrocarbon 1 mole PMA	0.5 mole Hydrocarbon 1 mole PMA	0.33 mole Hydrocarbon 1 mole PMA	.025 mole Hydrocarbon 1 mole PMA
31,32	Terphenyl	5.6×10^{10}			
33,34	Naphthalene	9.7×10^6	9.9×10^7		
35,36	Anthracene	8.3×10^5	7.9×10^5		
37,38	Phenanthrene	1.0×10^5		2.4×10^5	
39,40	Pyrene	1.6×10^4		3.5×10^5	
41,42,43	Chrysene	1.6×10^5		1.6×10^5	1.2×10^6
46,47	Tri phenyl Chloromethane	4.6×10^{11}		5.8×10^{11}	
48,49	Fluoranthrene	4.4×10^5		3.6×10^6	

Constant Polymerization Conditions

Time 24 hr.

Temperature 253°C

$\text{ZnCl}_2/\text{PMA} = 2/1$

TABLE VII

Effect of the Acid Anhydride
on Resistivity of PAQR Polymers

Samples	Hydrocarbon	Resistivity (Ω - cm)	
		1 mole Phthalic Anhydride	1 mole PMA
		1 mole Hydrocarbon	1 mole Hydrocarbon
60,33	naphthalene	3.2×10^5	9.7×10^6
61,35	anthracene	6.1×10^6	8.4×10^5
62,37	phenanthrene	8.4×10^6	1.0×10^5
63,39	pyrene	5.9×10^4	1.6×10^4
64,46	tri phenyl chloromethane	2.0×10^{12}	4.6×10^{11}
65,41	chrysene	8.6×10^5	1.6×10^5

Constant Polymerization condition: Temperature = 253°C,
time = 24 hr., 2 moles $ZnCl_2$ per mole anhydride.

Miscellaneous Acenes - The room temperature resistivities of several acenes, similar to anthracene in size and structure, but containing heteroatoms, were compared.

A polymer made with acridine exhibited similar resistivity to anthracene, while an anthraquinone PAQR polymer exhibited a markedly lower value. Values are presented in Table VIII.

TABLE VIII

Effect of Heteroatoms in the Acene

Acene	Polymerization		Room Temperature resistivity (ohm-cm)
	Temp. (°C)	Time (hr.)	
anthracene	306	24	1.8×10^5
acridine	306	24	6.8×10^5
anthraquinone	306	24	1.2×10^4

The introduction of a nitrogen in place of the gamma carbon would not be expected to radically affect intra-molecular conjugation, hence resistivity. Presence of the quinone groups on the acene could lead to a higher number of electrically unstable linkages in the polymer, or possibly to a side reaction consisting of fusion of quinones to give large ring systems for incorporation into the polymer.

3. THERMAL ACTIVATION ENERGY

Subsequent to the determination of room-temperature resistivities, several polymers representative of the entire series were selected for thermal activation studies.

Relationships between measurement temperature and resistivity were obtained at compaction pressures of 650 Kg/cm² and 1820

Kg/cm². The temperature range extended from approximately 25°C to 100°C.

It was determined that the logarithms resistivity of the polymers is a linear function of reciprocal temperature, in the range under study. Arrhenius plots for several PAQR polymers, at a compaction pressure of approximately 1800 Kg/cm², are shown in Figure 13.

Both thermal activation energy (E_a), and energy gap, (E_g), values were obtained for the series. The quantities are described by:

$$\rho = \rho_0 \exp. (E_a/KT)$$

$$\text{and } E_g = 2 E_a$$

where: ρ_0 = constant
 ρ = resistivity at T
 K = Boltzman constant

It should be noted that although the quantity E_g is utilized to describe the thermal activation behavior, adherence to the band theory is not implied⁶. The activation energy, or "energy gap" in organic semiconductors is probably a function of both intra and inter molecular barriers, and is therefore a composite of both. At present, justification for the use of E_g in describing polymeric organic semiconductors, lies only in the facilitation of comparison with other semiconductor systems.

Values of activation energy and ρ_0 , for representative PAQR polymers, are summarized in Table IX.

For the series of polymer measured, E_g values ranged from approximately 0.3 to 0.8 electron volts. Both E_g and ρ_0 generally

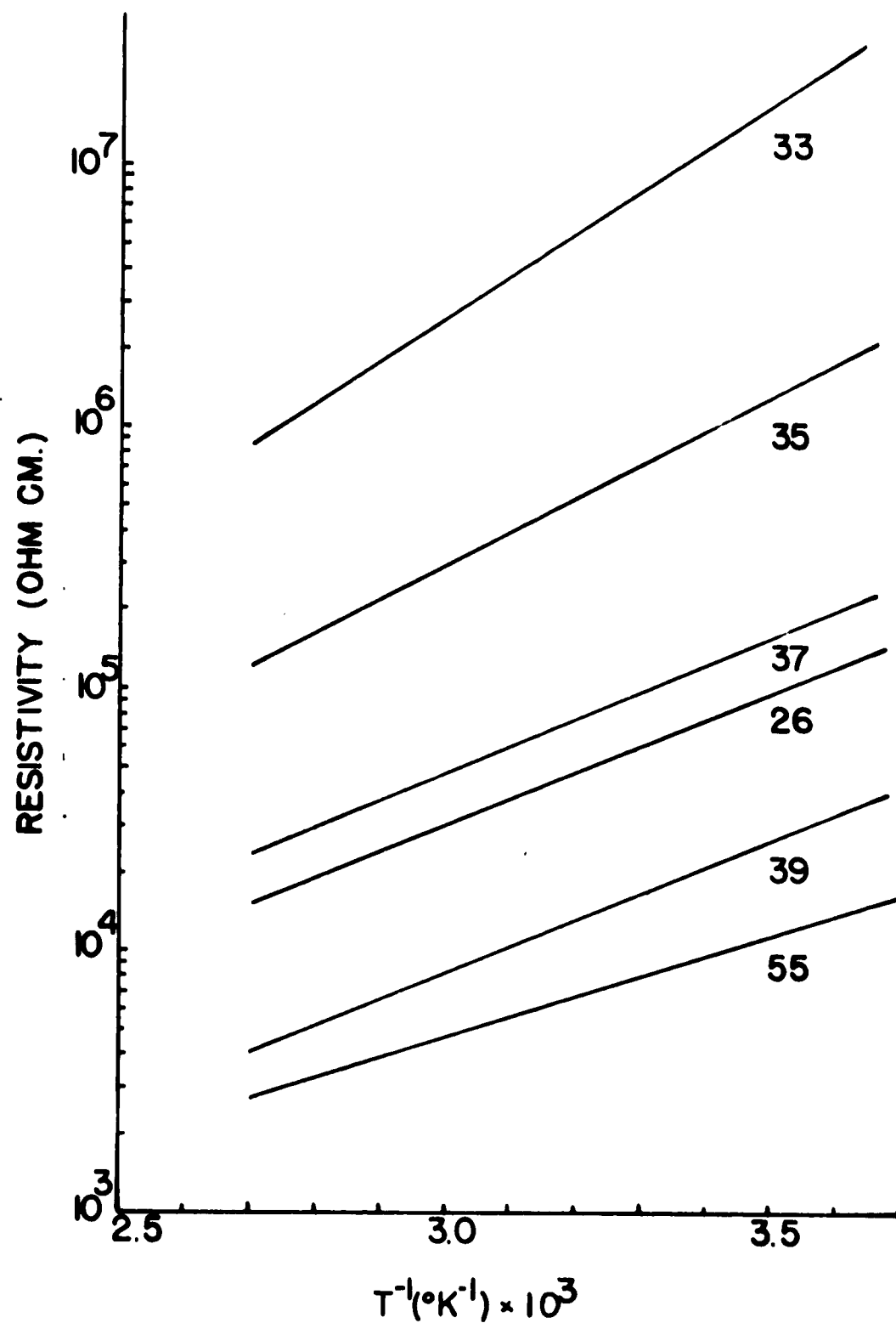


Figure 13, Resistivity Of Several PAQR Polymers As
A Function Of Measurement Temperature.

Curve Numbers Correspond To Polymers Described In
Tables 5 & 6

TABLE IX

Activation Energy (E_a) and Energy Gap (E_g)

Values for PAQR Polymers

Sample	Acene*	Resistivity (Ω -cm) 25°C	E_a (eV)			E_g (eV)			ρ_o
			1820 Kg/cm ²	650 Kg/cm ²	1820 Kg/cm ²	1820 Kg/cm ²	650 Kg/cm ²	650 Kg/cm ²	
26g	pyrolyzed, 26a	3.05×10^{-2}	0.001		ca. -0.002				
86	dibenzpyrene	9.5×10^2	0.206	0.202		0.413	0.404		1.1×10^7
55	pyrene (306°C)	7.6×10^3	0.155	0.165		0.310	0.329		5.5×10^6
39	pyrene (253°C)	1.6×10^4	0.198	0.197		0.395	0.395		7.1×10^7
26a	phenanthrene	6.7×10^4	0.198	0.191		0.397	0.382		3.0×10^8
37	phenanthrene	1.0×10^5	0.205	0.205		0.410	0.409		5.5×10^8
35	anthracene	8.3×10^5	0.257	0.259		0.515	0.519		4.7×10^{10}
33	naphthalene	9.7×10^6	0.322	0.324		0.644	0.647		8.3×10^{12}
66	triphenylmethane	5.8×10^{11}	0.420			0.840			3.3×10^{19}

* For polymerization conditions see Tables V and VI.

increased with increasing room temperature resistivity.

The relationship between E_g and the number of fused rings in the acene monomer is shown in Figure 14. A notable deviation from the general order was encountered with the dibenzpyrene polymer.

Although no distinguishable effect of compaction pressure on E_g was noticed here, as can be seen in Table IX, concurrent work with a similar polymer at pressures to 106,000 Kg/cm, indicates that a decrease of 1.7×10^{-6} eV. cm²/Kg might be expected⁴². This contribution, (.002 eV), would be indistinguishable in the limited pressure range studied here.

4. THERMOELECTRIC EFFECTS

The Seebeck coefficient, and related parameters were evaluated for seven PAQR polymers. Samples, with room temperature resistivities ranging from approximately 10^3 ohm cm to 10^6 ohm cm were measured; the maximum resistivity value being set by equipment limitations. Accuracy of the determinations was largely a function of the temperature differential at each measurement, and varied from approximately 2 to 15 percent as the temperature differential decreased from approximately 200°C to 20°C.

All of the polymers exhibited essentially linear relationships between the thermal gradient (ΔT) and the induced potential (ΔV). This permitted the development of a single-valued relationship between the Seebeck coefficient (Q) and the median sample temperature. The absolute Seebeck coefficients, Peltier coefficients and $\Delta V/\Delta T$ relationships for two representative PAQR polymers are shown in Figures 15 and 16.

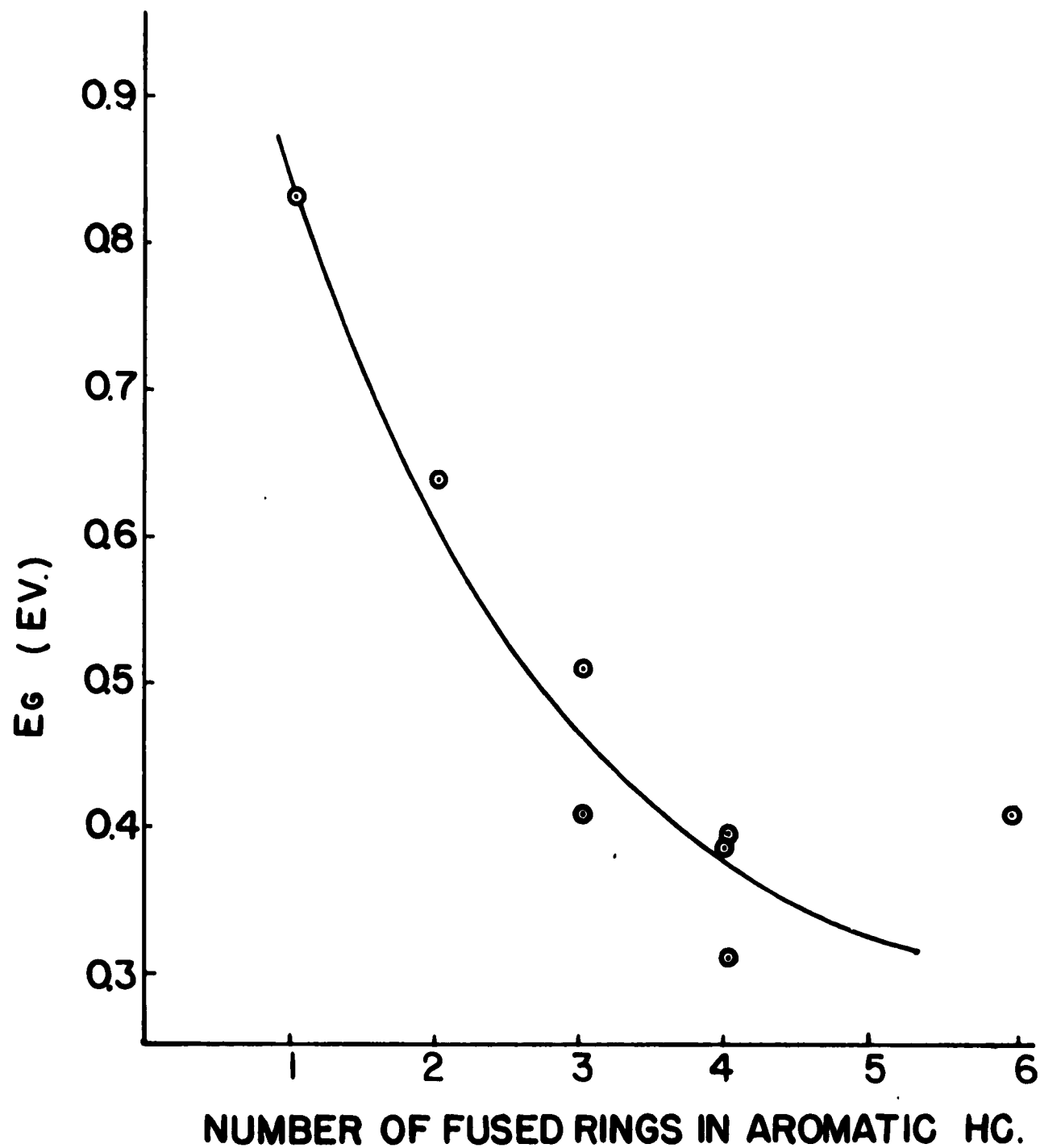


**Figure 14, "Energy Gap", (2×Activation Energy), As
A Function Of Monomeric Acene Size In
PAQR Polymers.**

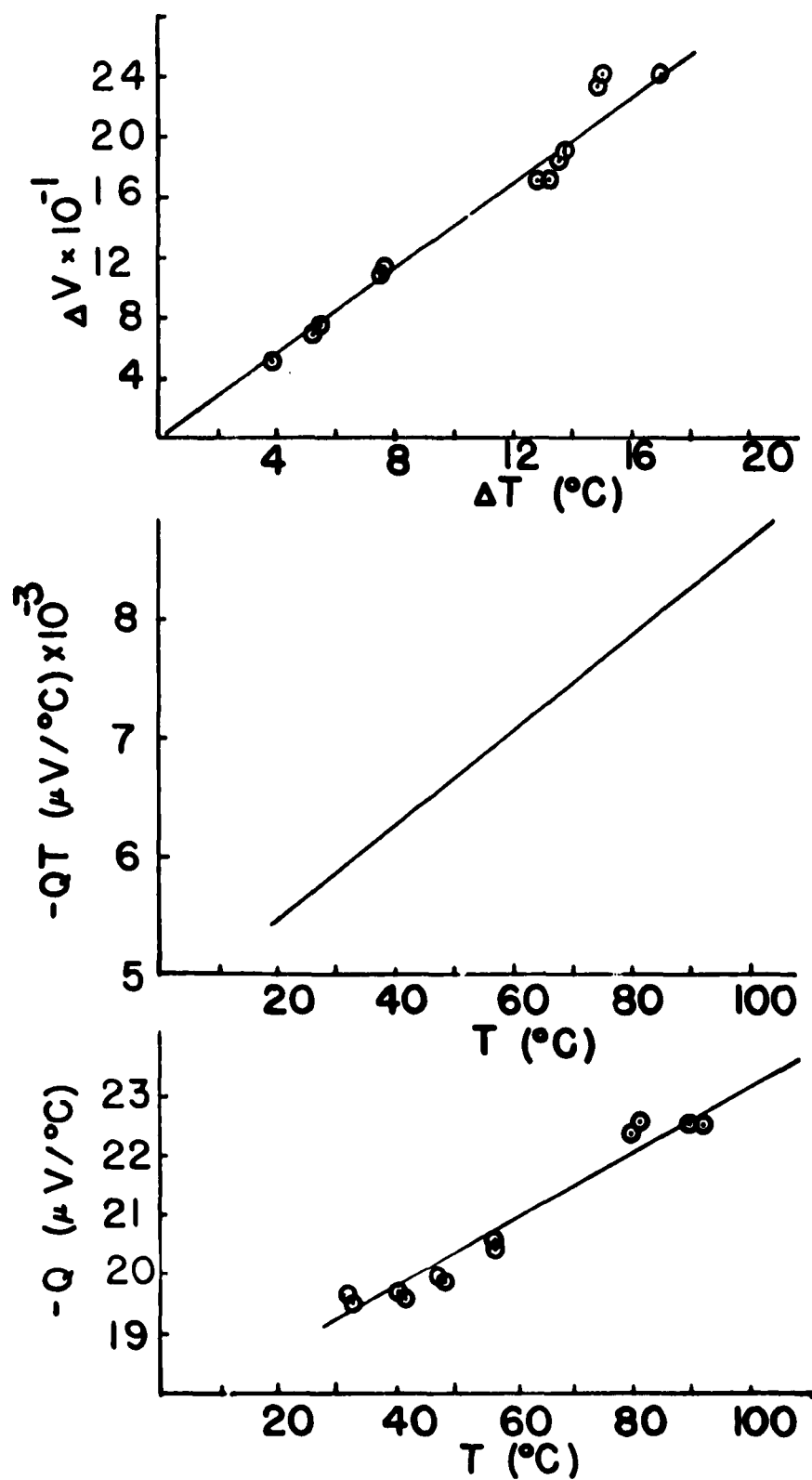


Figure 15, Thermoelectric Properties Of Polymer
86, 1:1:2, Dibenzpyrene : Pyromellitic
Dianhydride : ZnCl_2 .
 Q = Seebeck Coeff. QT = Peltier Coeff.

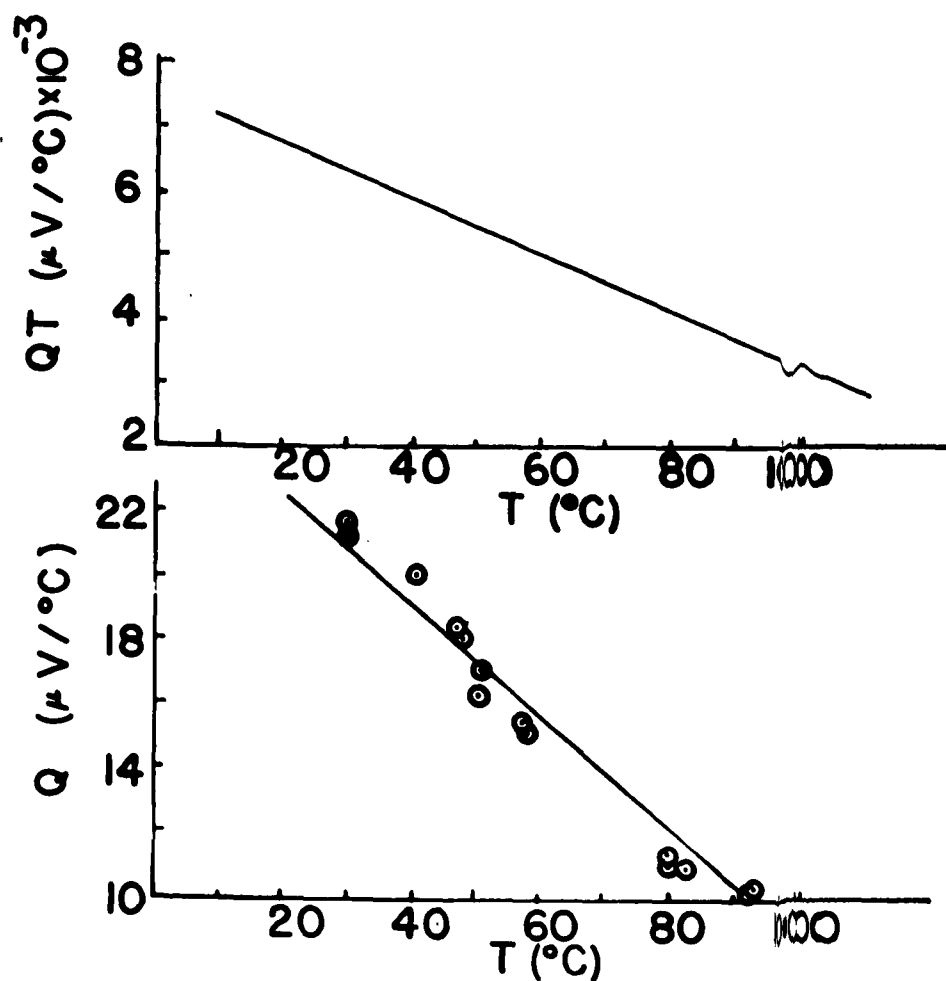
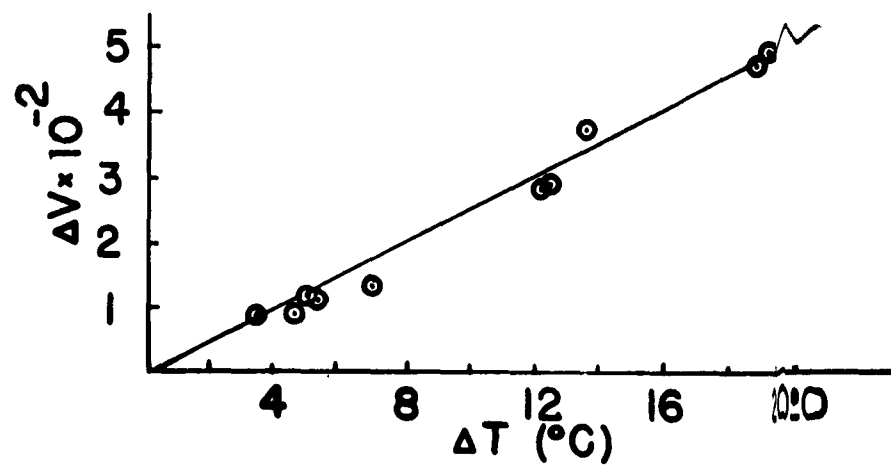


Figure 16, Thermoelectric Properties Of Polymer

39, 1:1:2, Pyrene : Pyromellitic

Dianhydride : $ZnCl_2$.

Q = Seebeck Coeff. QT = Peltier Coeff.

Seebeck coefficients, ranging from -19.0 to 345.5 microvolts per °C, were obtained with the measured PAQR series. The Seebeck values at 25°C are summarized in Table X.

It should be noted that all samples exhibited p-type conduction, with the exception of the dibenzpyrene PAQR polymer. This material, it might be noted, exhibited the lowest resistivity of the PAQR polymer series.

The Seebeck coefficient of the p-type materials declined slightly with temperature, in all observed cases, whereas the n-type polymer exhibited an increase. One may therefore conclude that the polymers all became more "negative" in carrier type as temperature increased. The temperature coefficient of Q was generally on the order of -1 microvolt per (°C)².

Although a trend toward higher Seebeck coefficient, with increasing room-temperature resistivity, is noted, a conclusive correlation was not obtained (Figure 17). The general validity of this trend is, however, supported by the results of Loebner, in his studies concerning the effect of pyrolysis temperatures (above 700°C) on the thermoelectric power of baked carbons²⁶.

The thermoelectric powers observed in this study are consistent with the values obtained on organic semiconductors, by other researchers. To place our results in perspective as to existing data, a general summary of thermoelectric values for organic semiconductors is presented below:

1. PAQR polymers = -19 to + 350 microvolts per °C (this study)
2. Poly copper phthalocyanine = + 15 to + 35 microvolts per °C (Epstein and Wild¹³)

TABLE X
Seebeck Coefficients of Several PAQR Polymers

Polymer No.	Acene *	Resistivity at 25°C, (ohm cm)	Q at 25°C (microvolts/°C)	d Q/dt (microvolts/°C/°C)
86	dibenzpyrene	9.5×10^2	-19.0	+ .55
55	pyrene	7.6×10^3	+69.6	- .90
39	pyrene	1.6×10^4	+21.8	-1.76
37	phenanthrene	1.0×10^5	+155.9	- .50
41	chrysene	1.6×10^5	+122.5	-6.87
35	anthracene	8.3×10^5	+345.5	-1.80
43	chrysene	1.2×10^6	+123.0	-6.85

* For polymerization conditions see Tables V and VI.

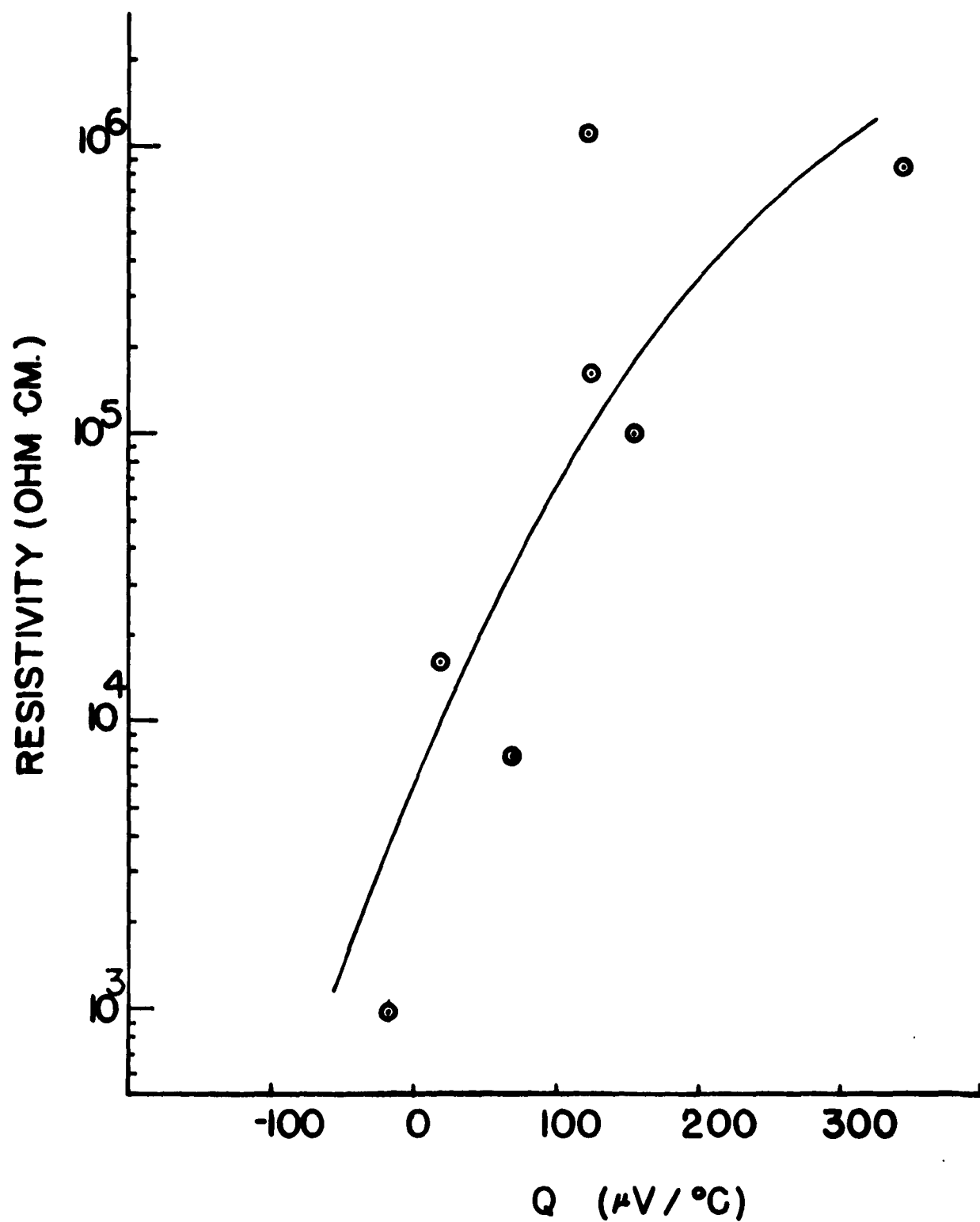


Figure 17, Seebeck Coefficient As A Function Of Resistivity_{25C}
In PAQR Polymers.

3. Xanthane polymer = +500 microvolts per °C
(McNeill and Weiss²⁷⁻⁸)
4. Phthalocyanine, metal-free, = +50 microvolts
per °C (Fielding and Gutman¹⁵)
5. Crystal Violet = -300 microvolts per °C
(Schroeder⁴³)
6. Molecular complexes = up to +1100 microvolts
per °C (Labes et al.^{21,22})
7. Phenolphthalein-type polymers = +50 to +500
microvolts⁴² per °C

Figure of Merit - The efficiency of semiconductors as thermoelectric devices depends on three interrelated material parameters; thermoelectric power, thermal conductivity and electrical resistivity. Figure of merit values for several PAQR polymers were calculated by the following expression:

$$Z = \frac{Q^2}{\rho k}$$

where Z = figure of merit
 Q = thermoelectric power
 k = thermal conductivity
 ρ = electrical resistivity

The thermal conductivity data were obtained by assumed analogy to recent work of Epstein and Wildi¹³ on poly copper-phthalocyanine. A value of 1×10^{-3} cal./cm. sec. °C was used in calculating the figure of merit.

Results are summarized in Table XI.

TABLE XI

Figure of Merit for Several PAQR Polymers

Polymer No.*	Q 25°C (microvolts per °C)	Figure of Merit (°C) ⁻¹ x 10 ⁺¹¹	
		25°C	100°C
86	-19.0	34	290
55	+69.6	65	150
39	+21.8	3.4	2.5
37	+155.9	26	110
35	+345.5	14	100

* For polymerization conditions, see Tables V and VI.

5. HALL COEFFICIENT

The apparatus, and technique employed for determination of the Hall coefficient was found to be generally inadequate for measurements on samples with resistivities encountered in the PAQR polymer series. Large asymmetry potentials, resulting from the high potentials required to pass sufficient carriers through the samples and from the difficulty in placing electrodes symmetrically prevented detection of the Hall voltage in most samples.

A reliable value was, however, obtained for sample 55, the PAQR polymer of pyrene and pyromellitic dianhydride (306°C). The Hall determination corroborated the results of thermoelectric power measurements, in that p-type conductivity was observed. The magnitude of the Hall coefficient, at room temperature was 288 cm³/coul.

This provides, in itself, almost certain proof that conduction in this polymer is electronic, and not ionic; for ionically conducting materials do not exhibit a detectable Hall voltage.

A rough estimate of the effective carrier density may be obtained by use of the following relationship:

$$N_h = (R_H eV)^{-1}$$

where N_h = The number of effective p-type carriers

R_H = The Hall coefficient

e = Electron charge

V = The velocity of light

From this equation, the effective number of carriers is estimated as $2 \times 10^{16}/\text{cm}^3$.

The mobility was estimated by the relationship:

$$\mu_H = R_H \sigma$$

where μ_H = Hall mobility

σ = conductivity = $7.6 \times 10^3 \text{ mho cm}^{-1}$

A value of $.04 \frac{\text{cm}^2}{\text{volt sec.}}$ was obtained.

Although the above values may have limited quantitative significance, they more or less establish that there are a minimum of 2×10^{16} carriers/ cm^3 in the polymer.

Somewhat higher carrier concentrations were found in poly copper phthalocyanine, in Hall coefficient determinations by Epstein and Wildi¹³. They estimated N_h at approximately $10^{18}/\text{cm}^3$.

6. ELECTRON SPIN RESONANCE

Estimates of the number of unpaired electrons in various PAQR polymers were obtained by measurement of electron spin density. The equipment and technique for obtaining quantitative results have been previously outlined.

A significant correlation between conductivity and unpaired electrons in PAQR polymer samples, was established. Figure 18 contains a plot of electron spin density at room temperature vs. the room-temperature sample resistivity.

The general level of unpaired spins in PAQR polymer samples ranged from approximately 10^{17} to 10^{20} spins/gm. It is interesting

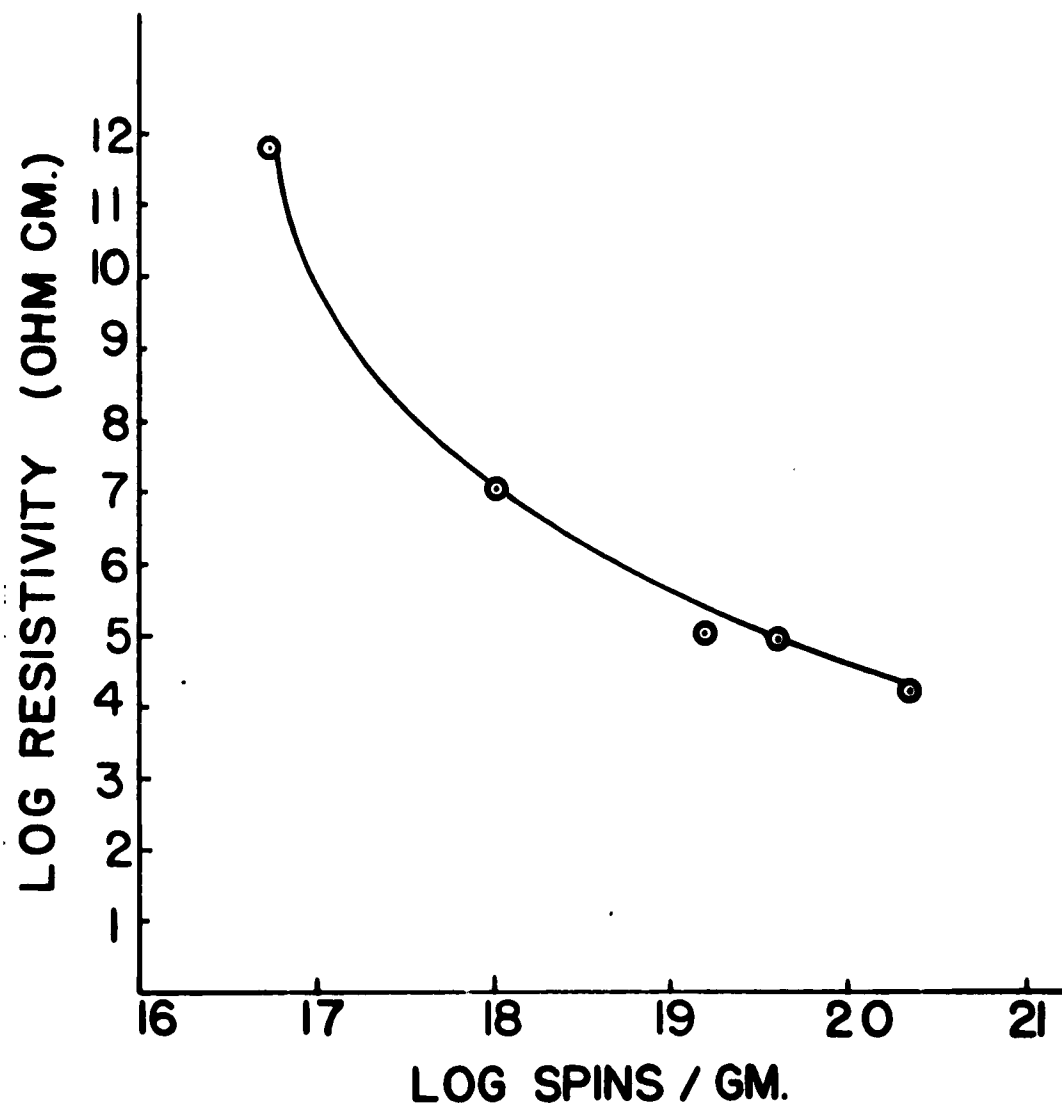


Figure 18, Electron Spin Density As A Function
Of Resistivity_{25C} In PAQR Polymers.

to compare these figures with the carrier concentration estimates from the Hall coefficient determinations in this study, and by Epstein and Wildi¹³, (poly copper phthalocyanine). As previously discussed, a minimum positive carrier concentration of approximately 3×10^{16} was estimated from our Hall determination. Epstein and Wildi estimated a minimum of 10^{16} to 10^{18} carriers/cc³⁵.

The number of unpaired spins, based on each repeating polymer unit, was calculated in the following manner:

$$\text{Spins / average polymer unit} = (\text{Spins/gm}) \times \\ (2 \text{ Mw. acene} \quad \text{Mw. PMA}) \times (6 \times 10^{23})^{-1}$$

The results, summarized in Table XII, indicate that larger acene nuclei are associated with more unpaired spins per average polymer unit. This is well within reason, since as the size of the acene incorporated in the polymer becomes larger, more free radicals can be stabilized by conjugation with the benzenoid structures. Figures showing the increase in resonance energy with acene size are available in ref. 55. The narrow electron spin resonance signals obtained are, in general, characteristic of unpaired delocalized electrons associated with a highly conjugated molecule.

7. MISCELLANEOUS ELECTRICAL CHARACTERISTICS

The conduction mechanism in PAQR polymers was found to be electronic. Using the measurement procedure outlined in the experimental section, a cumulative current of 4.5×10^5 coulombs per gram was passed through a polymer sample. The data contained in Table XIII show no significant change in resistivity subsequent to the passage of 4.7 gm equivalents 1 gm polymer.

TABLE XII

Electron Spin Density in PAQR Polymers

Sample *	Room temperature Resistivity (ohm cm)	Spins per gram	Approximate Spins Average polymer Unit	Peak Half Width, (Gauss)
66	5.8×10^{11}	5.0×10^{16}	6.6×10^{-5}	8
33	9.7×10^6	1.5×10^{18}	1.1×10^{-3}	5.75
37	1.0×10^5	1.5×10^{19}	1.3×10^{-2}	5
39	1.6×10^4	1.9×10^{20}	1.9×10^{-1}	3.5
26	6.6×10^4	6.5×10^{19}	5.8×10^{-2}	4.25

* Polymerization conditions in Tables V and VI.

TABLE XIII

Resistivity of a PAQR Polymer as a
Function of Cumulative Current *

Time (hr)	Potential (Volts)	Average Current (Amps)	Ratio, R sample** to R control	Cumulative Current (Coulombs/gm) x 10 ⁻⁴
0	48	0.29	0.99	
0.5	48	0.29	0.99	0.43
5.5	48	0.28	0.97	4.57
16.0	48	0.26	0.97	12.6
19.0	48	0.25	0.96	14.9
19.5	48	0.28	0.97	15.2
22.5	48	0.26	0.97	17.5
39.5	48	0.25	0.95	30.0
60.5	48	0.24	0.98	45.0

* Sample #25, phenantrene, 250°C

** To within Temperature correction error

Scatter in the resistivity data is primarily due to slight compaction and temperature differences between the sample and the control polymer. On the basis of polymer structure, approximately 1.1 gm equivalent should have been sufficient to electrolyze all of the O and H atoms.

On this basis, if ionic conduction were significant, it would have easily been detected by this experiment.

In addition to the electronic nature of the polymers, no polarization was evident from visual observations of current increase or decrease on applying or removing a potential. The measurements were, however, limited by the response of the meters, and more refined techniques such as high frequency a.c. measurements were not employed.

The above coulombic evidence, together with that obtained on determination of a large Hall coefficient, prove quite conclusively that electronic and not ionic conduction takes place in these PAQR polymers.

The resistance of a representative PAQR polymer was found to vary nonlinearly with the applied field strength. High relative precision was achieved by comparison of the polymer sample with metallic (ohmic) resistors in a Wheatstone bridge. Potentials applied across the bridge ranged from 1.55 to 52 volts, corresponding to a potential range of .78 to 26 volts across the polymer sample. The resistivities from three independent determinations are presented in Figure 19. A reduced expression for resistance was employed, for convenience of comparison between samples. The

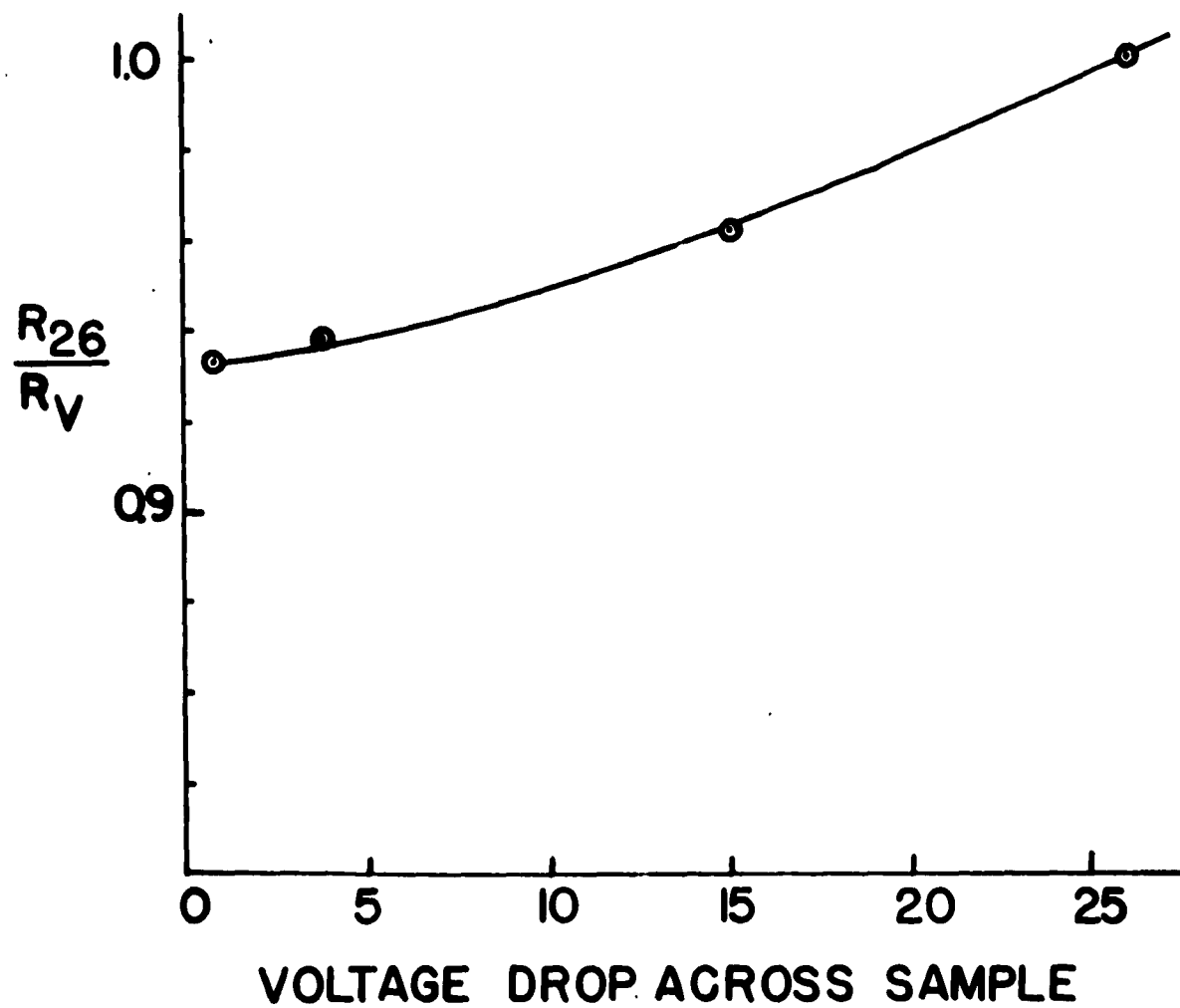


Figure 19, Effect Of Applied Potential On The Resistance
Of A PAQR Polymer (Polymer 39)

abscissa is plotted in terms of:

$$\frac{R_{26}}{R_V} = \frac{\text{Resistance at a potential drop of 26V}}{\text{Resistance at a potential drop of } x \text{ V}}$$

8. THERMAL AND CHEMICAL TREATMENTS

Samples of a PAQR polymer were heated in a helium atmosphere, to temperatures approaching 1200°C. Each sample was treated for 1/2 hour, under helium. The relationship between heat treatment temperature and resistivity (measured at room temperature) is shown in Figure 20. Conductivity was found to go through a minimum at approximately 500°C, showing that the original synthetic structure of the PAQR polymers is unique and thermally sensitive and is not that of a pyropolymer.

At temperatures in excess of 600°C, it is probable that extensive changes in the polymer structure occur, due to the volatilization of H, CO and CO₂, etc.

The electron spin resonance characteristics of the 1000°C treated polymer were quite different from those of the PAQR materials. A very faint resonance was observed with a peak half-width of approximately 1200 Gauss, as opposed to the high concentration of spins responding in a peak half-width field variation of only 3 to 5 Gauss. This is indicative of gross changes in conduction mechanism, since the interaction of free carriers has increased markedly.

Obvious changes in polymer composition are also reflected by the analysis of the 1000°C heat treated polymer.

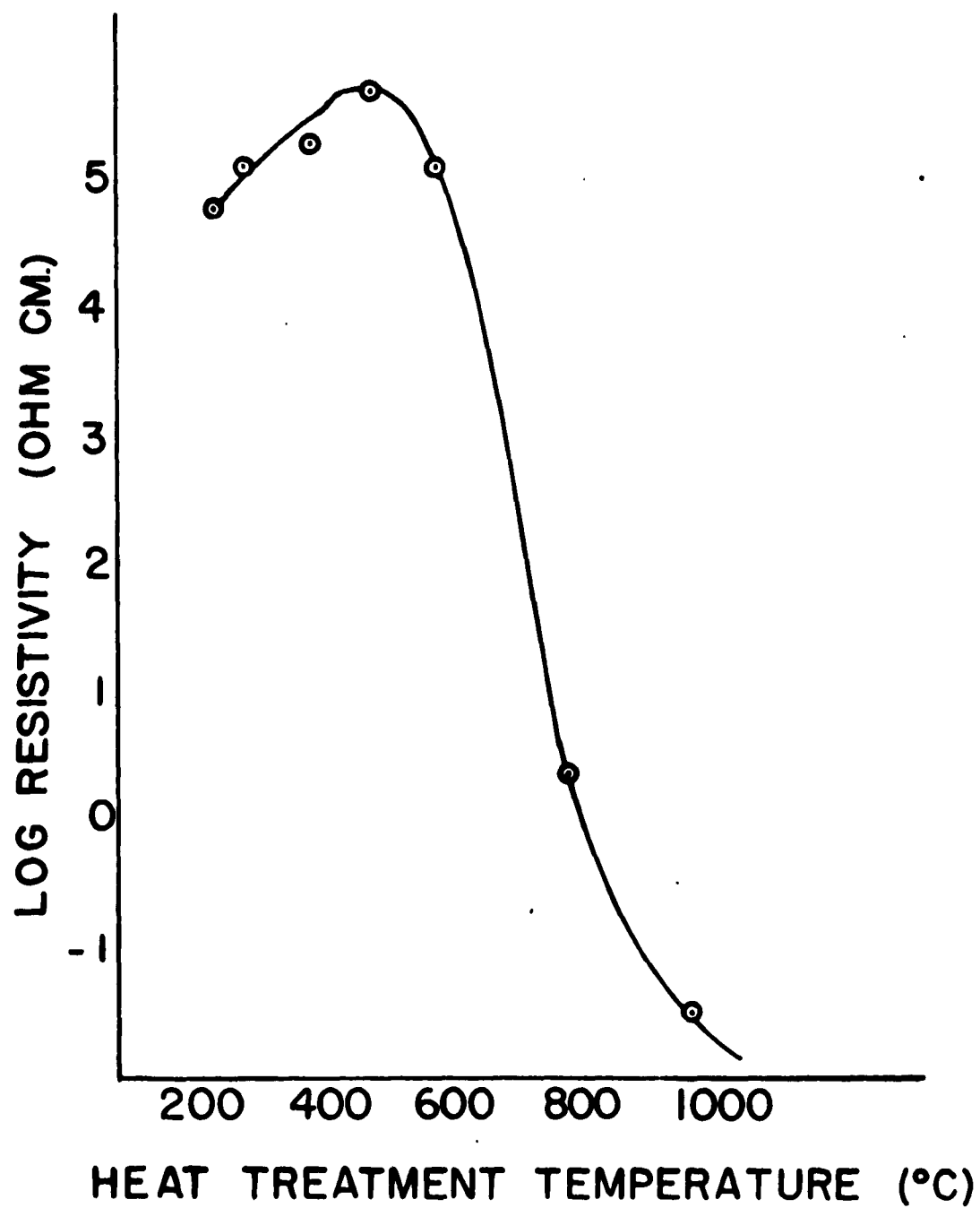


Figure 20, Effect Of Post Treatment Temperature,
(In He), On The Resistivity_{25C} Of A
PAQR Polymer (Polymer 26)

	<u>C</u>	<u>O</u>	<u>H</u>
Sample 26	84.48	7.21	3.52
Sample 26 (heated to 1000°C)	96.45	1.32	1.37

The heat treated sample had a negative temperature conductivity coefficient (Table IX), and was a degenerate semi-metal.

Rather interesting results were obtained when a PAQR polymer was subjected to comparatively low temperature thermal treatments, under various environments. When PAQR polymers were heat treated, in air, at temperatures ranging from 50°C to 250°C, the resistivity of the polymers increased as a function of treatment time. The relationship between heat treatment temperature-time and resistivity of a PAQR polymer is shown in Figure 21.

After 100 hours at 250°C, the polymer became essentially an insulator. The rate of increase in resistance, with time, is presented in Figure 22.

A sample which was heated in vacuum at 250°C for 100 hours, was relatively unaffected by the heat treatment, whereas a sample heated under otherwise identical conditions, but in the presence of air finally exhibited a room temperature resistivity in excess of 10^{10} ohm cm.

The increase in resistivity was found to be only slightly reversible. This was determined by reheating a sample, which had previously been heated to 250°C in air, in a vacuum ampule, under similar conditions. The reheating decreased the sample resistance from 10^{10} to 10^9 , whereas the untreated polymer had a

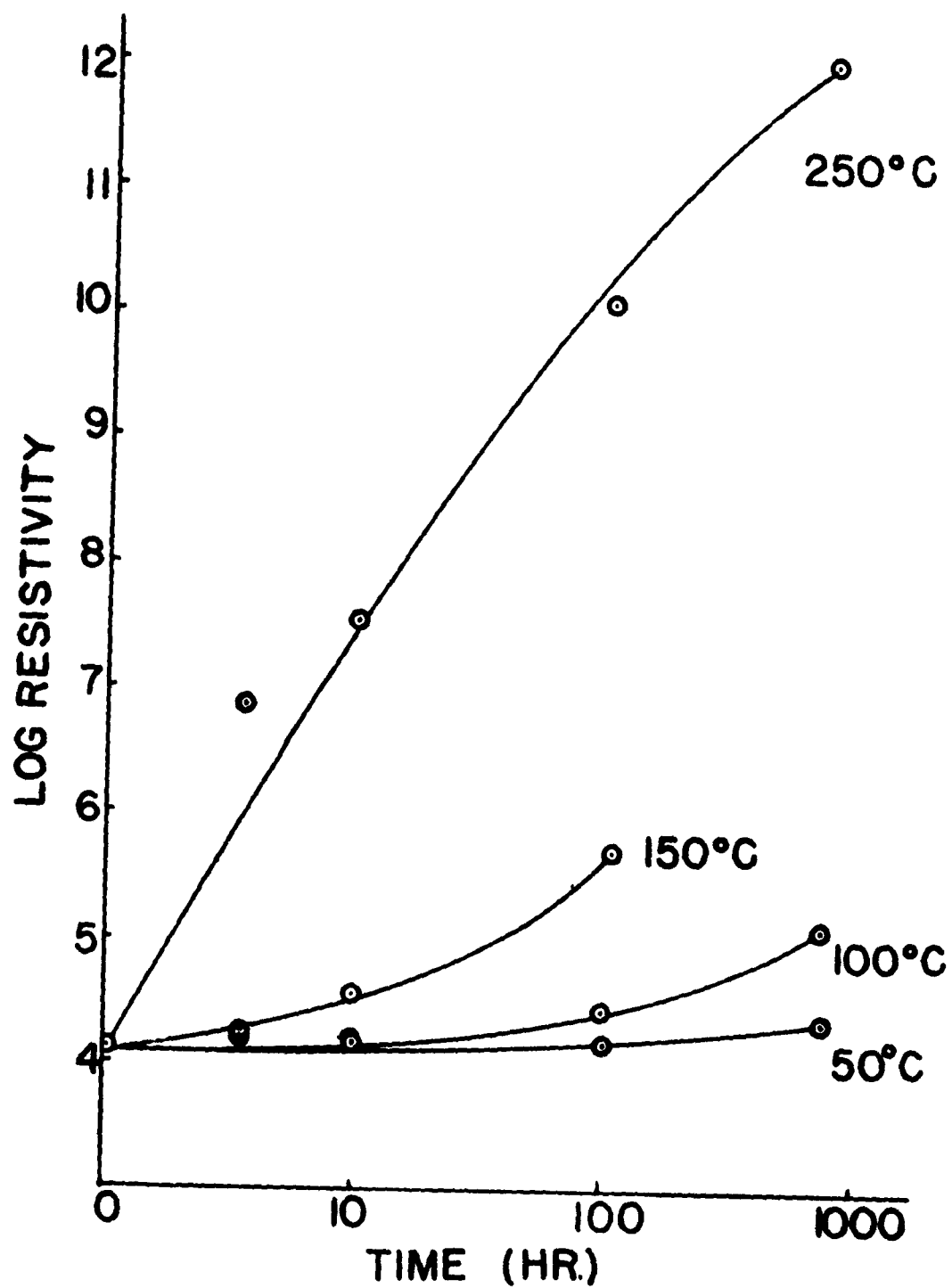


Figure 21, Effect Of Post Treatment Temperature,
(In Air), On The Resistivity_{25C} Of
A PAQR Polymer (Polymer 39)

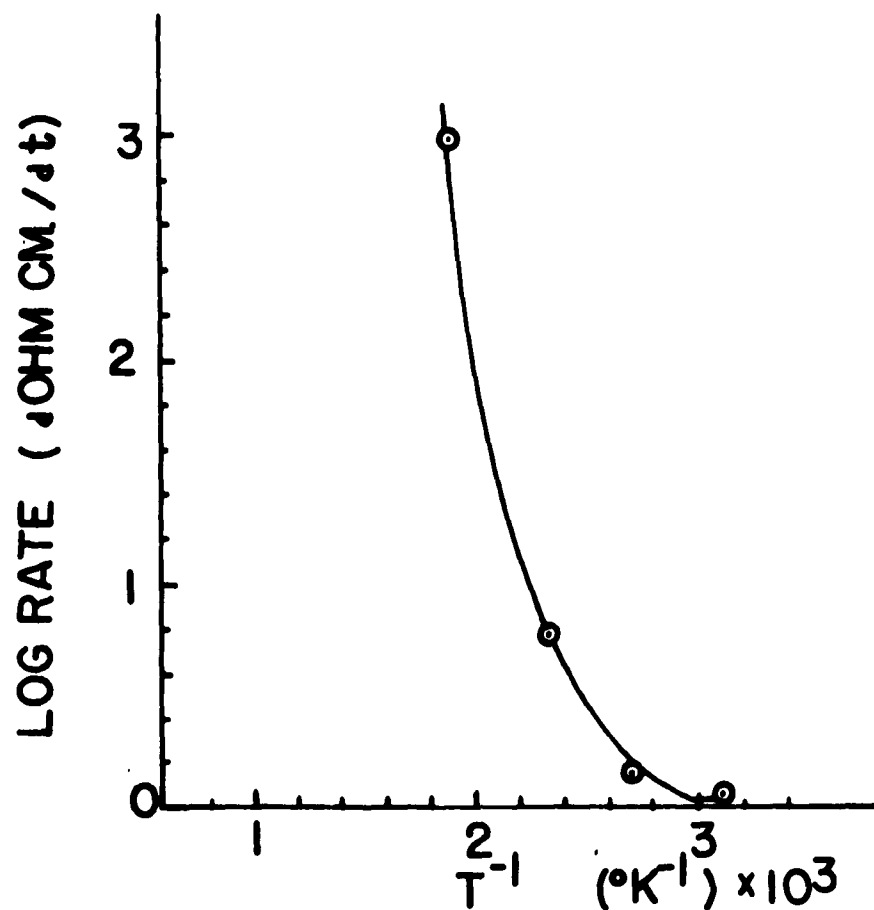


Figure 22, Rate Of Resistivity Increase In A PAQR Polymer, (Post Treated In Air), As A Function Of Post Treatment Temperature. (Polymer 39)

resistivity of 10^4 ohm cm. The latter change probably indicates a partial reversal of the chemi-sorption of oxygen.

Carbon, hydrogen, and oxygen analyses on the materials strongly indicate that the addition of oxygen to the structure is involved in the depression of conductivity. Analyses of several heat treated samples are presented in Table XIV. Assuming no carbon losses, the increases in oxygen level correspond to 3×10^{20} and 7×10^{21} atoms per gram of polymer. Comparison of electron spin densities shows that the assimilation of oxygen by the polymers corresponds to a definite reduction in spin concentration (Table XV).

Similar heat treatments on several pyro polymers at low temperature, (250°C), produced no noticeable changes in resistivities in the temperature range under study.

Further studies of the conductivity mechanism were pursued by observation of the effect of various chemical modifications on polymer resistivity.

A significant reduction in conductivity was observed when MEK hydroperoxide was reacted with a PAQR polymer. Reaction with an inorganic redox system seemed also to increase resistivity. The bulky DPPH radical, applied as a dilute solution in diethyl ether, had no detectible effect on conductivity properties.

Treatment with a saturated solution of sodium bisulfite, (reducing agent), seemed to actually improve conductivity, whereas the action of an inorganic oxidizing agent lowered the conductivity somewhat. Data are summarized in Table XVI.

TABLE XIV

Effect of Heat Treatment in Air on Polymer Composition

<u>Heat Treatment</u>	<u>mole % C</u>	<u>mole % H</u>	<u>mole % O</u>
none	63.4	30.6	6.0
10 hr at 250°C	64.7	28.6	6.7
725 hr at 250°C	59.0	21.0	20.0

TABLE XV

Effect of Heat Treatment on Electron Spin Resonance

<u>Treatment</u>	<u>Log Resistivity</u>	<u>Spins/gm</u>	<u>est. Oxygen Uptake Molecules/gm</u>
none	4.16	1.9×10^{20}	
air, 10 hr at 250°C	7.51	3.4×10^{19}	3×10^{20}
air, 725 hr at 250°C	11.97	$\ll 10^{15}$	7×10^{21}
vacuum, 100 hr at 250°C	4.50	9.2×10^{19}	

TABLE XVI

Effect of Chemical Treatment on Resistivity

Polymer Sample	Post Treatment	Resistivity (ohm cm)
56	None	2.1×10^4
56	Water, 18 hr, RT	2.5×10^4
56	Saturated NaHSO_3 , 18 hr, RT	8.7×10^3
56	Saturated KClO_3 , 18 hr, RT	3.0×10^4
56	Mixture NaHSO_3 & KClO_3 , 18 hr, RT	4.4×10^4
56	ether	2.2×10^4
56	ether + MEK hydroperoxide	9.3×10^4
56	ether + DPPH	1.8×10^4

TABLE XVII

Bromination of PAQR Polymers

Sample*	Untreated Resistivity (ohm cm.)	Resistivity after Bromination (ohm cm.)	Molecules of Bromine assimilated (molecules/gm)
33	9.7×10^6	3.7×10^8	3.15×10^{21}
37	9.1×10^4	6.3×10^6	6.31×10^{21}
39	1.6×10^4	6.3×10^5	5.23×10^{21}
59	3.8×10^5	2.2×10^7	6.15×10^{21}

* Polymerization conditions - see Tables V and VI.

Addition of bromine to PAQR polymers increased the resistivity markedly. Samples of several polymers were treated with liquid bromine for approximately three hours at room temperature. After careful washing and removal of unreacted bromine, the polymers were found to have assimilated approximately 10^{21} molecules of bromine per gram. A decrease in conductivity of two orders of magnitude was attributable to the bromine assimilation. Data are summarized in Table XVII. The electron spin density of sample 39 was found to decrease from 1.9×10^{20} spins/gm to 2.9×10^{19} spins/gm with the addition of bromine. Interaction between unpaired electrons increased on chemical treatment, as evidenced by broader ESR peaks (Figure 23).

It is interesting to note the similarity in conductivity and spin concentration behavior with oxygen and bromine addition.

Direct reaction with free radicals, or a general decrease in resonance energy of the acene components, due to an addition reaction across double bonds, may have been responsible for the observed depression of conductivity, etc.

The discrepancy between the number of assimilated molecules and the electron spin densities might be due to the fact that the absolute accuracy of spin densities is an order of magnitude too low, or possibly that all of the atoms added to the polymer are involved in destroying conjugation consequential to conduction. The latter explanation, involving the concept of "eka-conjugation" to be clarified later, appears more attractive.

9. PHOTOELECTRIC PROPERTIES

The investigation of photoelectric properties, as has been previously mentioned, was carried out in a rather crude apparatus,

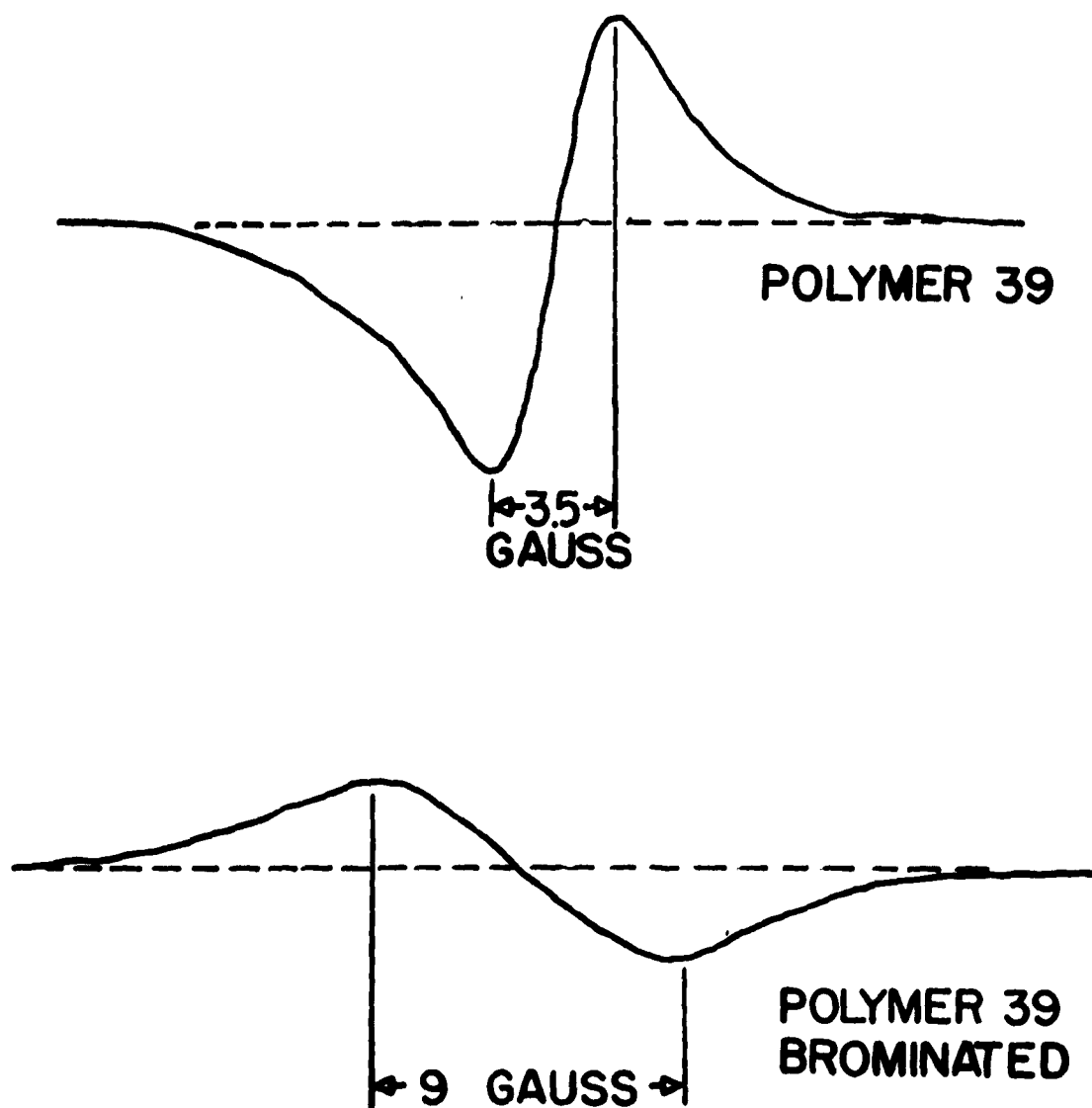


Figure 23, Electron Spin Density Differential Curves
For Polymer 39, Untreated; And Polymer 39,
Subsequent To Bromination.

and results are at best only semiquantitative. They nevertheless do indicate that the PAQR polymers exhibit photoconductivity and a photo-EMF. The technique employed in this study was inadequate for determination of carrier velocity, etc., and only served to gain some ideas as to the lifetime and extent of photo-excited carriers.

When a sample of polymer number 55, was illuminated through the transparent conducting tin oxide (NESA) window, a generally linear increase in voltage, to approximately 9 millivolts, was observed. The time required to reach a maximum was approximately 0.8 minutes.

After maintaining illumination for 1.2 minutes at the equilibrium photo EMF, the source was turned off and the voltage was observed to decay to a minimum within 0.8 minutes. The photo EMF curve for polymer #55 is shown in Figure 24.

Measurement of the photo current showed no corresponding maximization after 0.8 minutes. The photo current steadily increased over a period of approximately 2 minutes to a maximum of 0.5 millimicro amperes, after which the illumination was terminated. When irradiation was terminated, an exponential decrease in current was observed, over a period of approximately 0.8 minutes.

Considering the sample resistance, (3×10^6 ohms), and the steady state photo EMF, (9×10^{-3} volts), a maximum photo current of approximately 3 millimicro amperes was anticipated.

The change in sample resistivity was determined by applying a potential of 1.5 volts and measuring the change in current upon illumination. When the light source was turned on, a steady increase in current was observed, over a period of ca. 0.9 minutes.

1- LIGHT ON
2- LIGHT OFF

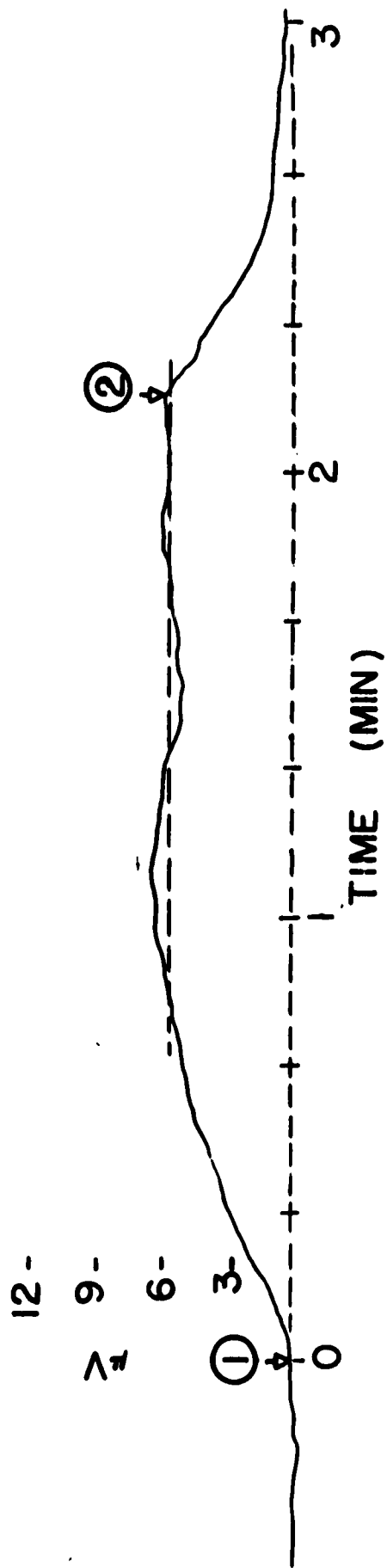


Figure 24, Photovoltaic Curve For A PAQR Polymer (Polymer35)

The steady state current corresponded to a resistivity decrease (assuming approximately ohmic behavior) of approximately six percent. A decay time of approximately 1.1 minutes was observed subsequent to removal of the illumination.

D. ALUMINUM CHLORIDE CATALYZED PAQR POLYMERS

Several polymers were synthesized at relatively low temperatures, using aluminum chloride as a catalyst, and pyromellitoyl chloride as the acylating agent. The polymers all exhibited resistivities several orders of magnitude higher than the zinc chloride catalyzed materials.

At the temperatures employed, the lactone formation reaction should have been relatively minor.

The acid chloride can exist as either 1,2,4,5 benzene tetracarboxyl chloride or as isomeric 3,3' dichloroisobenzobis furanones, lower temperatures generally favoring the former, which leads to quinone formation.

Resistivities of the polymers were determined on samples, as synthesized, and subsequent to heating in the presence of SOCl_2 . Results are summarized in Table XVIII. The ethanol and benzene soluble fractions exhibited higher resistivities than the insoluble polymeric material.

Polymerization of pyromellitoyl chloride with bi and, terphenyl produced yellow-tan, insoluble, infusible materials. The fused-nuclei acenes generally yielded deeply purple-black polymers, indicating a lower molecular weight and/or lower level of conjugation than experienced with the zinc chloride catalyzed polymers. This situation is reflected in the higher resistivities encountered with the aluminum chloride catalyzed materials.

TABLE XVIII

	Acene	Resistivity (ohm cm)	Resistivity After SOCl ₂ Treatment (ohm cm)	Resistivity of ZnCl ₂ Catalyzed PAQR (ohm cm)
I & J	Biphenyl	9.1×10^{11}	(decomposed to tar) 10^4	3.4×10^{10}
C & D	Terphenyl	6.2×10^{11}	2.8×10^{11}	1.4×10^7
G & H	Naphthalene	1.6×10^{12}	6.7×10^{11}	1.4×10^6
A & B	Anthracene	1.5×10^8	2×10^9	3.2×10^5
E & F	Phenanthracene	7.8×10^{11}	4.9×10^{11}	1.0×10^5

E. REACTION OF QUINONES AND DIISOCYANATES

Several quinones were condensed with diisocyanates at a 1:1 molar ratio. The monomers were polymerized at 250°C and 300°C.

At the temperatures employed, the starting materials liquified immediately, and turned, first deep brown then black.

After a short period, generally 15 minutes at 250°C and 4 minutes at 300°C, a rapid evolution of CO₂ was observed and the mass solidified. The reaction time was quite reproducible. Polymers were left at reaction temperature for certain periods after the solidification occurred. The materials were, in all cases, deep brown to black solid, insoluble, infusible materials. Resistivities were generally above 10¹¹ ohm cm. Carbon, hydrogen, oxygen analysis of a polymer sample indicated that the desired highly conjugated structure was not attained, since oxygen did remain in the sample. C = 77.33%, H = 4.01%, N = 4.43%, O = 11.05%. Results are summarized in Table XIX.

F. POLYACENES

A mixture of polymeric materials was obtained when tetrabromobenzene was acylated with sodium potassium alloy. The polymers were generally reddish-black.

After separation of the ethanol soluble, benzene soluble, and insoluble fractions, resistivities were measured. Results are summarized in Table XX.

TABLE XIX

Polymers of Quinones and Di-isocyanates

	Monomers	Temperature °C	Solidification Time (min.)	Total polymeri- zation time (hr)	Resistivity
101	1,4 Naphthaquinone + TODI	100	no polymer		
102	1,4 Naphthaquinone + TODI	100	no polymer		
103	1,4 Naphthaquinone + TODI	250	15	18.25	4.6×10^{11}
104	1,4 Naphthaquinone + TODI	250	15	1.25	2.5×10^{11}
105	1,4 Naphthaquinone + TODI	250	15	.25	2.5×10^{11}
106	1,4 Naphthaquinone + TODI	306	4	18	5.9×10^{11}
110	1,4 Naphthaquinone + TODI	306	4	4 (min)	6.7×10^{11}
113	Anthraquinone + TODI	306	50	1	6.5×10^{11}
114	Anthraquinone + TODI	306	50	19	6.2×10^{11}
115	Paraquinone + TODI	256	23	18	5.6×10^{11}
116	Paraquinone + TODI	306	8	18	4.7×10^{11}

TODI = p - Toluenedi-isocyanate

TABLE XX

<u>Fraction</u>	<u>Description</u>	<u>Room Temperature Resistivity (ohm cm)</u>
ethanol soluble	thermoplastic	1.2×10^{12}
benzene soluble	thermoplastic	6.0×10^{11}
insoluble	infusible	2.6×10^{11}

G. ANILINE BLACK POLYMER

The resistivity of the aniline black material, synthesized as previously described in the experimental section, was found to be 3×10^{10} ohm cm at 25°C. A deep violet-black color was observed in this polymer, indicating a low degree of molecular weight and/or, conjugation.

H. THEORETICAL INTERPRETATIONS

As has been previously discussed, the organic semiconductors do not meet the criteria for the rigid application of simple band theory in interpreting their electronic behavior. It was, nevertheless, of interest to determine the electronic parameters in several PAQR polymers, on the assumption that the models did apply.

The theoretical development of band theory, and pertinent equations are described in Cusack⁹. Equations, relating the thermoelectric power to the carrier parameters, such as number and mobility, have been derived by V. A. Johnson and K. Lark-Horovitz^{17,18}.

Parameters have been derived, assuming intrinsic behavior, (number of positive carriers = number of negative carriers), and extrinsic, or impurity behavior (one carrier type predominates).

In intrinsic non-degenerate semiconductors, the Seebeck coefficient⁵⁴ can be described by:

$$Q = \frac{K}{e} \frac{(C-1)}{(C+1)} \left[\frac{E_g}{2kT} + 2 \right]$$

where Q = Seebeck coefficient
 K = Boltzman constant
 e = charge on an electron
 E_g = energy gap
 T = absolute temperature
 $C = \mu_o'/\mu_h'$ = ratio of mobilities, electrons to holes.

This can be rearranged to give:

$$C = \frac{-QT + E_g/2 + 2KT}{QT + E_g/2 + 2KT}$$

The mobilities can be calculated by:

$$\mu_h' = \frac{\sigma}{e n' (c+1)}$$

$$\mu_e' = c \mu_h'$$

where σ = conductivity

μ_h' = mobility of positive carriers

μ_e' = mobility of negative carriers

n' = number of positive carriers $\approx \frac{(2\pi M_h' KT)^{3/2}}{h^2} \times \exp(-E_g/2KT)$

where h = Planck's constant

M_h' = effective mass of carrier

Since the carrier mass could not be determined, the mass of an electron at rest was substituted.

Carrier parameters based on the intrinsic model are presented in Table XXI.

TABLE XXI

Carrier Parameters Based on the Intrinsic Model
(Band Theory) - From Thermoelectric Data

Polymer	Room temperature Resistivity (ohm cm)	$C = \frac{\mu_e}{\mu_h}$	$N_h^1 \times 10^{-15}$ (cm^{-3})	$\mu_h^1 \times 10^3$ ($\frac{\text{cm}^2}{\text{V. Sec.}}$)	$\mu_e^1 \times 10^3$ ($\frac{\text{cm}^2}{\text{V. Sec.}}$)
86	9.5×10^2	1.04	8.3	390	4.1×10^{-1}
55	7.6×10^3	0.82	60.0	7.5	6.2×10^{-3}
39	1.6×10^4	0.95	11.0	18.0	1.7×10^{-2}
37	1.0×10^5	0.69	8.3	4.5	3.1×10^{-3}
35	8.3×10^5	0.47	1.2	4.3	2.1×10^{-3}

TABLE XXII

Carrier Parameters Based on the Impurity Model
(Band Theory) - From Thermoelectric Data

Polymer	$N_h^1 \times 10^{-20}$ (cm^{-3})	$\mu_h^1 \times 10^{-8}$ ($\frac{\text{cm}^2}{\text{V. sec}}$)
86	2.3	270
55	4.1	200
39	2.4	160
37	11.	5.7
35	100	.075

Compared with the electron spin density and chemical treatment results, the carrier concentration values are several orders of magnitude lower.

Assuming extrinsic non-degenerate behavior, the Seebeck coefficient may be represented by:

$$Q = \pm \frac{k}{e} \left\{ 2 - \ln \left[\frac{n_h h^3}{2(2\pi M_h^* kT)^{3/2}} \right] \right\}$$

This can be rearranged to give:

$$n_h = \frac{2(2\pi M_h^* kT)^{3/2}}{h^3} \exp\left(2 + \frac{Qe}{k}\right)$$

Mobility can be calculated by:

$$\sigma = n_h e \mu$$

where σ = conductivity

Carrier parameters based on the extrinsic model are presented in Table XXII. If we calculate the number of impurities, on the basis of this model, a value in excess of 10^{24} cm^{-3} is obtained; hence the model is certainly inapplicable.

Eka - Conjugation and Enhanced Electronic Behavior.

As an alternative to the simple band model approach in considering the semiconducting polymers, we have used the following working hypothesis. There is now appreciable evidence that when the size of a set of conjugated double and single bonds is larger than some number (about 10 to 15 double-single bond pairs) then the molecule acquires unusual characteristics. It is to be expected that the formation of the biradical state (exciton) will then become easy. For ease of reference, we have termed this re-

quired degree of conjugation as eka-conjugation. Eka-conjugation may be said to exist when the degree of conjugation becomes such that the extent of biradical (or similar exciton) formation becomes appreciable at room temperature. The energetics of the transition may be semi-quantitatively considered by the 'electron-in-a-box' model. Representing the biradical as $\cdot R \cdot$, and its eka-conjugated precursor as R, we may write



$$(2) \quad (\cdot R \cdot)(R)^{-1} = K_1 = \exp(-\Delta F_1/RT)$$

$$(3) \quad \Delta F_1 = \Delta H_1 - T\Delta S_1 \approx {}^3E$$

where 3E is the energy of conversion to the triplet state biradical. From the electron-in-a-box-model, we may set as a fair approximation,

$$(4) \quad {}^3E \approx E_{n=2} - E_{n=1} = \frac{\pi^2 \hbar^2 (n_2^2 - n_1^2)}{e m a^2}$$

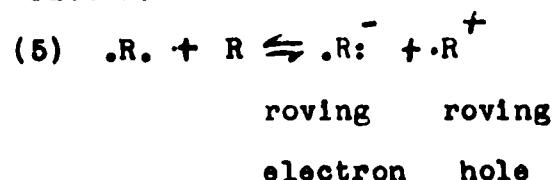
$$\approx \frac{14.42}{x^2} ; [\text{in eV}]$$

where $a = (1/2)(2L_0x) = L_0x$

$L_0 = \text{C} \text{---} \text{C}$ bond length = ca. 1.40Å

x = number of mers

The ion pair forming reaction from which the carriers result may be written:



$$(6) \quad \frac{(\cdot R \cdot^-)(\cdot R^+)}{(\cdot R \cdot)(R)} = K_2 = \exp(-\Delta F_2/RT)$$

By this argument, we will expect to have an "intrinsic-type" semiconductor where

$$(7) \quad (.R: \bar{\cdot}) = (R^{\cdot}) = n_e \approx n_h = n_1,$$

and we may set $(.R.) = s/2 \approx 1/2$ the concentration of observable spins per cm^3 .

Combining, we get

$$(8) \quad 2 M_i^2 / s(R) = K_2$$

$$(9) \quad m_i = \frac{s}{2} \exp \left[-\frac{\Delta F_2 + \Delta F_1}{2 kT} \right] \approx \frac{s}{2} \exp \left(\frac{-\Delta F_2 + \frac{3}{2} E}{2 kT} \right) \\ = (R) \exp \left[-\frac{\Delta F_2 - \Delta F_1}{2 kT} \right] \approx (R) \exp \left[\frac{-\Delta F_2 - \frac{1}{2} E}{2 kT} \right]$$

where n_1 is the number of either mobile electrons or mobile holes acting as carriers.

As discussed elsewhere at greater length⁴⁰, there is reason to expect the mobility to occur by way of hopping processes, where E_s is the saddle height energy for the hopping process, and

$$(10) \quad u = (\text{const.}) T^2 \exp (-E_s/kT)$$

In the event that there is a cooperative process between the carriers and excitons, a factor of $(n_{1x}/n_1 + n_{1x})$ must be included, and the new $E_s' < E_s$. Recalling that the eka-conjugated structures are large and assymetrical, as well as highly polarizable, it will be expected that some field dependence of the conductivity will result. The eka-conjugation model appears to account qualitatively and occasionally semiquantitatively for the various attributes previously mentioned for the PAQR polymers. Further study of this interesting area is actively in progress.

CONCLUSIONS

1. Highly conjugated semiconducting polymers are produced by the condensation of a poly-acene with pyromellitic dianhydride in the presence of zinc chloride, and at temperatures of approximately 200 to 400°C. Conductivities with a range of 10^{-2} to 10^{-10} mho cm^{-1} are obtained by varying the type and concentration of aromatic hydrocarbon in the polymer.

2. Activation energies in the PAQR polymers fall within a range of 0.1 to 0.5 eV, and are generally a direct function of room temperature resistivity.

3. The PAQR series synthesized in this study exhibit a range of Seebeck coefficients of from minus 19 to plus 345 microvolts per °C. As the temperature increases, the Seebeck coefficient, hence the carrier type, seems to become more "negative".

4. The conduction mechanism in PAQR polymers is electronic, as evidenced by electrolysis experiments, and the existence of a relatively large Hall coefficient. Nonohmic behavior has been established by comparison of polymers with an ohmic resistor in a Wheatstone bridge.

5. A semiquantitative relationship between electron spin density and conduction, has been established in PAQR polymers. This indicates that the conductivity level in polymers of this type is predominantly a function of the number of free carriers, rather than of carrier mobility. However, the slightly higher spin interactions generally observed with decreasing conductivity may reflect that mobility changes can be considered as minor participants in determining conductivity.

6. The PAQR polymers have a dissimilar structure and mode of conduction from that of the pyropolymers.

7. The narrow electron spin peak-halfwidths, observed in PAQR polymers, are characteristic of unpaired, delocalized electrons, along the chain of conjugation.

APPENDIX I

ELECTRON SPIN RESONANCE CALCULATIONS

(1) Conditions

Modulation = 1 Gauss
 Scanning Speed = 15 Gauss/min.
 Incident power = 100 milliwatts
 DC current supply = 5 microamps

(2) Standard sample

$$\text{Spins} = \frac{\text{wt. (gm)} \times 6.023 \times 10^{23} \text{ (spins)}}{394 \frac{\text{gm}}{\text{mole}}} = S_0$$

(3) Spin densities

$$\# \text{Spins} = S_0 \times \frac{W_1}{W_{01}} \times \frac{W_2}{W_{02}} \times \frac{Q_0}{Q} \times \frac{G_0}{G}$$

where S_0 = spins in standard sample

W_0 = peak-to-peak width in the standard scan

W_1 = peak-to-peak width in the sample scan

W_2/W_{02} = amplification correction

Q_0 = cavity geometry loss factor (standard)

Q = cavity geometry loss factor (sample)

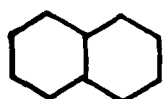
G_0 = gain setting on amplifier with standard

G = gain setting on amplifier with sample

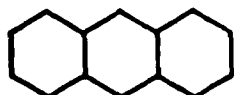
The electron spin density was then calculated as spins/gram:

Spins/gram = #Spins/weight of polymer sample

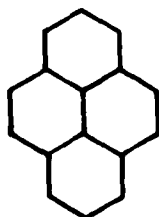
APPENDIX II



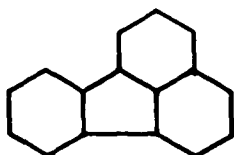
NAPTHALENE



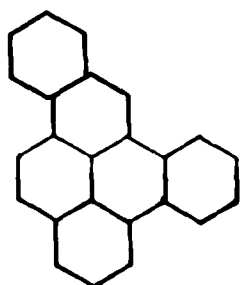
ANTHRACENE



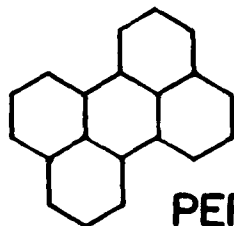
PYRENE



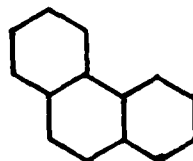
FLUORANTHRENE



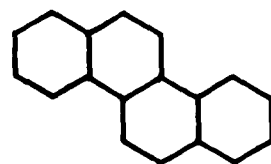
1,2,4,5, DIBENZPYRENE



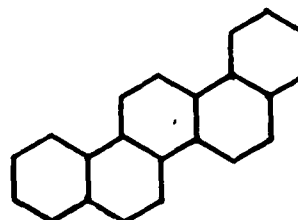
PERYLENE



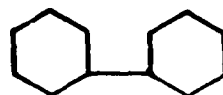
PHENANTHRENE



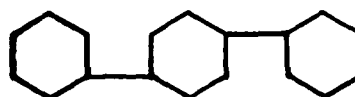
CHRYSENE



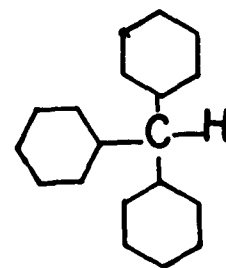
PICENE



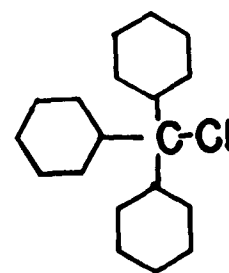
BI PHENYL



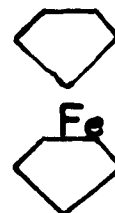
TER PHENYL



TRIPHENYLMETHANE



TRIPHENYLCHLORO-
METHANE



FERROCENE

REFERENCES

1. Akamatsu, H., and Inokuchi, H., Solid State Physics, 12, ed. by F. Seitz and D. Turnbull, Academic Press, (1955).
2. Akamatsu, H., Inokuchi, H., and Matsunaga, Y., Bull. Chem. Soc., Japan, 29, 213 (1956).
3. Akamatsu, H., Kagaku to Kogyo (Tokyo), 11, 607-13 (1958).
4. Berlin, A.A., Khim. Teknol. Polymerov., 7-8, 139-58 (1960)
Translation in English by H.N. Friedlander, Standard Oil Information Division, Translation TR 60-122.
5. Bohrer, J.J., Trans. N.Y. Acad. Sci., 20, 367-82 (1958).
6. Bornmann, J.A., and Pohl, H.A., "Further Studies on Some Semi-conducting Polymers", Plastics Laboratory Technical Report 63A, Sept. 1961 (Princeton University, 1961).
7. Brown, G.P., and Aftergut, S., "Investigation of Organic Semiconductors", WADC Tech. Report, 59-469, Sept. 1960.
8. Cook, J.W., and Hewett, C.L., J. Chem. Soc., 1933, 398.
9. Cusack, N., The Electrical and Magnetic Properties of Solids, Longmans Green and Co., Ltd., (1958).
10. Edwards, G.A., and Goldfinger, G., J. Polymer Sci., 16, 589 (1955).
11. Eley, D.D., Research, 12, 293-9 (1959).
12. Eley, D.D., Inokuchi, H., and Willis, M.R., Discussions Faraday Soc., 28, 54 (1960).
13. Epstein, A., and Wildi, B.S., J. Chem. Phys., 32, 324 (1960).
14. Feimayer, W., and Wolf, I., J. Electrochem. Soc., 105, 141-5 (1958).
15. Fielding, P.E., and Gutman, F., J. Chem. Phys., 26, 411-9 (1957).
16. Garrett, C.G.B., Chapter on 'Organic Semiconductors', in Semiconductors, ed. by N. B. Hannay (Reinhold, 1959).
17. Johnson, V.A., and K. Lark-Horowitz, Phys. Rev., 92, 226 (1953).
18. Johnson, V.A., Progress in Semiconductors, Vol. I, (Heywood and Co., 1956).

19. Kommandeur, J., and Hall, F.R., J. Chem. Phys., 34, 129-33 (1961).
20. Kommandeur, J., and Singer, L.S., *ibid.*, 34, 133-40 (1961).
21. Labes, M.M., Sehr, R., and Bose, M., *ibid.*, 32, 1570-2 (1960).
22. Labes, M.M., Sehr, R., and Bose, M., p. 47, Semiconduction in Molecular Solids, (Proc. of the Princeton Conf.) ed. by H.A. Pohl (Ivy-Curtis Press, 1960).
23. Laherrere, J.P., and Pohl, H.A., pp. 93-123, *ibid.*
24. Leblanc, O.H., and Huggins, C.M., Nature, 186, 552 (1960).
25. Lieser, T., and Nischk, G., Ann. Chem. Liebigs, 569, 66-74 (1950).
26. Loebner, E.E., Phys. Rev., 84, 153 (1951); errata, 86, 1056 (1952).
27. McNeill, R., and Weiss, D.E., Australian J. Chem., 12, 643-56 (1959).
28. McNeill, R., and Weiss, D.E., pp. 281-90, Proc. Fourth Conf. on Carbon (Pergamon Press, 1960).
29. Marschalk, C.M., Bull. Soc. Chem., 9, 400 (1942).
30. Mrozowski, S., Phys. Rev., 85, 609 (1952); errata, 86, 1056 (1952); 92, 1320 (1953).
31. Mrozowski, S., J. Chem. Phys., 21, 492 (1953).
32. Oster, G., Oster, G., and Kryszewski, M., Nature, 191, 164 (1961).
33. Packer, J., and Vaughn, J., Organic Chemistry, (Clarendon Press, London, 1958).
34. Pohl, H.A., pp. 241-57, Proc. Fourth Conf. on Carbon, (Pergamon Press, 1960).
35. Pohl, H.A., and Laherrere, J.P., *ibid.*, pp 259-65.
36. Pohl, H.A., pp. 9-24, Semiconduction in Molecular Solids, (Proc. of the Princeton Conf.) ed. by H.A. Pohl (Ivy-Curtis Press, 1960).
37. Pohl, H.A., and Rosen, S.A., Proc. Fifth Conf. on Carbon (Pergamon Press, London, 1960). (in press).
38. Pohl, H.A., Chem. Eng., 68, 104 (1961).
39. Pohl, H.A., Electro-Technology, 67, 85 (1961).

40. Pohl, H.A., "Semiconduction in Polymers", Plastics Laboratory Tech. Report, 61D, (Princeton Univ., 1961); also: Chapter in Modern Aspects of the Vitreous State, ed. by J.D. Mackenzie (Butterworths, in press).
41. Pohl, H.A., Bornmann, J.A., and Itoh, W., "Semiconducting Polymers", Plastics Laboratory Tech. Report, 60C, (Princeton Univ., 1961), cf. J. Electrochem. Soc., in press.
42. Pohl, H.A., and Opp, D.A., Abstracts of Papers Presented at Chicago, Ill., Sept. 1961, Div. Phys. Chem., Amer. Chem. Soc., p 32-3.
43. Schroeder, C., Master's Thesis, Ohio State Univ. (1952).
44. Speight, E.A., Stevenson, A., and Thorpe, J.F., J. Chem. Soc., 125, 2185 (1924).
45. Terenin, A., Proc. Chem. Soc., 1961, 321-9 (1961).
46. Thiele, J., and Wanschmidt, A., Ann. Chem. Liebigs, 376, 269 (1910).
47. Turkevich, J., p. 85, Semiconduction in Molecular Solids, (Proc. of Princeton Conf.), ed. by H.A. Pohl, (Ivy-Curtis Press, 1960).
48. Vartanyan, A.T., Acta Physicochim. URSS, 22, 201 (1947).
49. Wheland, G.W., Resonance in Organic Chemistry, Wiley and Sons, (1955).
50. Wilk, M., Z. Electrochem., 64, 930 (1960).
51. Winslow, F.H., Baker, W.O., and Pape, N.R., J. Polymer Sci., 16, 101 (1955).
52. Winslow, F.H., Matreyek, W., and Yager, W.A., Ind. Carbon and Graphite, p. 190 (1958).
53. Wilson, A.H., Theory of Metals, p. 207, 2nd Ed., Cambridge Univ. Press (1953).
54. Winterstein, A., Vetter, H., and Schoen, K., Ber., 68, 1079 (1953).

PRINCETON UNIVERSITY
Distribution List for Technical Reports
Contract DA-36-039-SC-89143

1n. Commanding Officer
Office of Naval Res. Branch Office
The John Crerar Library Building
86 East Randolph Street
Chicago 1, Illinois (1)

2n. Commanding Officer
Office of Naval Res. Branch Office
346 Broadway
New York 13, New York (1)

3n. Commanding Officer
Office of Naval Res. Branch Office
1030 E. Green Street
Pasadena 1, California (1)

4n. Commanding Officer
Office of Naval Res. Branch Office
Navy No. 100
Fleet Post Office
New York, New York (7)

5n. Director, Naval Res. Lab.
Washington 25, D. C.
Attn: Technical Inform. Officer (6)
Chemistry Division (2)
Code 6110 (1)

6n. Chief of Naval Research
Department of the Navy
Washington 25, D. C.
Attn: Code 425 (2)

7n. Technical Library OASD(R&D)
Pentagon Room 3E1065
Washington 25, D. C. (1)

8n. Technical Director
Research & Engineering Div.
Office of the Quartermaster General
Department of the Army
Washington 25, D. C. (1)

9n. Research Director
Chemical & Plastics Division
Quartermaster Res. & Eng. Command
Natick, Massachusetts (1)

10n. Air Force
Office of Scientific Res.(SRLT)
Washington 25, D. C. (1)

11n. Commanding Officer
Diamond Ordnance Fuze Labs.
Washington 25, D. C.
Attn: Tech. Ref. Section
(ORDTL 06.33) (1)

12n. Office of Chief of Staff(R&D)
Department of the Army
Pentagon 3B516
Washington 25, D. C.
Attn: Chemical Adviser (1)

13n. Chief, Bureau of Ships
Department of the Navy
Washington 25, D. C.
Attn: Code 340 (2)

14n. Chief, Bur. of Naval Weapons
Department of the Navy
Washington 25, D. C.
Attn: Technical Library (3)
Code RRMA-3 (1)

15n. ASTIA
Document Service Center
Arlington Hall Station
Arlington 12, Virginia (10)

16n. Command. Officer
USASRDL
Fort Monmouth, New Jersey
Attn: SIGRA/SL-RE (1)

17n. Naval Radiological Defense
Laboratory
San Francisco 24, California
Attn: Technical Library (1)

18n. Naval Ordnance Test Station
China Lake, California
Attn: Head, Chem. Div. (1)
Code 40 (1)
Code 50 (1)

19n. Commanding Officer
U.S. Army Research Office
Box CM, Duke Station
Durham, North Carolina (1)
Attn: CRD-AA-IP-Mr. Ulsh

20n. Brookhaven National Lab.
Chemistry Division
Upton, New York (1)

21n. Atomic Energy Commission
Research Division
Chemistry Branch
Washington 25, D. C. (1)

22n. Atomic Energy Commission
Library Branch
Technical Information ORE
Post Office Box E
Oak Ridge, Tennessee (1)

23n. U.S. Army Chem. Warfare Labs.
Technical Library
Army Chemical Center, Maryland (1)

24n. Office of Technical Services
Department of Commerce
Washington 25, D. C. (1)

25n. Commanding Officer
Naval Air Development Center
Johnsville, Pennsylvania
Attn: Dr. Howard R. Moore (1)

26n. Mr. M. Lipnick
Diamond Ordnance Fuze Laboratory
Washington 25, D. C. (1)

27n. Naval Powder Factory
Indian Head, Maryland
Attn: Mr. A. F. Johnson (1)

28n. Naval Electronics Laboratory
San Diego, California (1)

29n. Naval Ordnance Laboratory
Silver Springs, Maryland
Attn: Dr. Albert Lightbody (1)

30n. Materials Laboratory
New York Naval Shipyard
Brooklyn, New York (1)

31n. Commander
Mare Island Naval Shipyard
Rubber Laboratory
Vallejo, California (1)

32n. Naval Air Experiment Station
Philadelphia Naval Shipyard
Philadelphia 12, Pa. (2)

33n. Dr. J. H. Faull, Jr.
72 Fresh Pond Lane
Cambridge, Mass. (1)

34s. Dr. Gregg Andrus
OC Sig. O, R&D Division
Washington 25, D. C.
Attn: SIGKD 4A (1)

35n. Dr. A. V. Tobolsky
Department of Chemistry
Princeton University
Princeton, New Jersey (1)

36n. Dr. W. Heller
Wayne State University
Detroit, Michigan (1)

37n. Dr. U. P. Strauss
Department of Chemistry
Rutgers University
New Brunswick, New Jersey (1)

38n. Dr. E. G. Rochow
Department of Chemistry
Harvard University
Cambridge 38, Mass. (1)

39n. Dr. E. G. Wallace
Stauffer Chemical Company
1375 S. 47th Street
Richmond, California (1)

40n. Dr. R. S. Stein
Department of Chemistry
University of Massachusetts
Amherst, Mass. (1)

41n. Dr. H. C. Brown
Department of Chemical Engineering
Engineering & Ind. Exper. Station
University of Florida
Gainesville, Florida (1)

42n. Mr. J. B. Rust
Hughes Aircraft Company
Culver City, California (1)

43n. Dr. Leo Mandelkern
National Bureau of Standards
Washington 25, D. C. (1)

44n. Stauffer Chemical Company
Molded Products Division
3211 E. 26th Street
Los Angeles 23, California
Attn: Dr. John McColgan (1)

45n. Dr. G. Barth-Wehrenalp
Pennsalt Chemicals Corporation
P. O. Box 4388
Philadelphia 18, Pa. (2)

46n. Commanding Officer & Director
U.S. Naval Civil Engineering Lab.
Port Hueneme, California
Attn: Chemistry Division (1)

47n. Dr. T. G. Fox
Mellon Institute
4400 Fifth Avenue
Pittsburgh 13, Penna. (1)

48n. Dr. Riley Schaeffer
Department of Chemistry
Indiana University
Bloomington, Indiana (1)

49n. Library
Textile Research Institute
P. O. Box 625
Princeton, New Jersey (1)

50n. Plastics Tech. Eval. Center
Picatinny Arsenal
Dover, New Jersey (1)

51s. Commanding Officer
Engineer R&D Labs.
Fort Belvoir, Virginia
Attn: Document Center (1)

52s. Commanding Officer
U.S. Army Signal R&D Lab.
Fort Monmouth, New Jersey
Attn: SIGRA/SL-ADT (1)

53s. Commanding Officer
U.S. Army Signal R&D Lab.
Fort Monmouth, New Jersey
Attn: SIGRA/SL-ADJ (File Unit No. 3,
ECR Dept.) (1)

54s. Commanding Officer
U.S. Army Signal R&D Lab.
Fort Monmouth, New Jersey
Attn: SIGRA/SL-TN (FOR RETRANS-
MITTAL TO ACCREDITED BRITISH & (3)
CANADIAN GOVERNMENT REPRESENTATIVES)

55s. Commanding Officer
U.S. Army Signal Equip. Support Agcy.
Fort Monmouth, New Jersey
Attn: SIGMS/ADJ (1)

56s. Commanding Officer
U.S. Army Signal Equip Support Agcy.
Fort Monmouth, New Jersey
Attn: SIGMS-SDM (1)

57s. Commanding Officer
U.S. Army Signal R&D Lab.
Fort Monmouth, New Jersey
Attn: SIGFM/EL-P (1)

58s. Commander
Air Force Command & Control Div.
Air R&D Command
U.S. Air Force
L.G. Hanscomb Field
Bedford, Mass.
Attn: CROTIR-2 (1)

59s. Commander
Rome Air Development Center
Air R&D Command
Griffiss AFB, New York
Attn: RCSSID (1)

60s. Commanding Officer
U.S. Army Signal R&D Labs.
Fort Monmouth, New Jersey
Attn: SIGRA/SL-PE (1)

61s. Commanding Officer
U.S. Army Signal R&D Labs.
Fort Monmouth, New Jersey
Attn: SIGRA/SL-PEM (1)

62s. Advisory Group on Electronic
Parts

Moore School Building
200 South 33rd Street
Philadelphia 4, Pa. (4)

63s. Commanding General
Army Ordnance Missile Command
Signal Office
Redstone Arsenal, Alabama (1)

64s. General Electric Company
Research Laboratory
P. O. Box 1088
Schenectady, New York
Attn: Dr. A. M. Bueche (1)

65s. Tech. Information Center
Lockheed Missiles & Space Div.
3251 Hanover Street
Palo Alto, California
Attn: Mr. W. A. Kozumplik (1)

66s. U.S. Army Signal Liaison Office
Aeronautical Systems Division
ATTN: ASDL-9

Wright-Patterson AFB, Ohio (2)

67s. USNSRD, Facilities
Clothing & Textile Division
3rd Avenue & 29th Street
Brooklyn 32, N.Y. (Librarian) (1)

68s. C. O. USASRDL
Fort Monmouth, New Jersey
Attn: SIGRA/SL-XE
Dr. H. H. Kedesdy (1)

69s. C. O. USASRDL
Fort Monmouth, New Jersey
Attn: SIGRA/SL-PDP
Dr. H. Mette (1)

70s. Chief, U.S. Security Agcy.
Arlington Hall Station
Arlington 12, Virginia (2)

71s. Deputy President, U.S.A.
Security Agency Board
Arlington Hall Station
Arlington 12, Virginia (1)

72s. Space Technology Labs.
P. O. Box 95001
Los Angeles 45, California (1)

73s. Dr. M. S. Cohen, Chief
Propellants Synthesis Section
Reaction Motors Division
Denville, New Jersey (1)

74s. Boeing Airplane Company
Transport Division
P. O. Box 707
Renton, Washington
Attn: Mr. F.N. Markey, Unit Chief (1)

75s. Commanding Officer
Ordnance Materials Res. Office
Watertown Arsenal
Watertown 72, Mass.
Attn: RPD (1)

76s. Commanding Officer
Rock Island Arsenal
Rock Island, Illinois
Attn: Mr. R. Shaw, Laboratory (1)

77s. Monsanto Chemical Company
Research & Engineering Div.
Boston 49, Massachusetts
Attn: Mr. K. Warren Easley (1)

78s. R. R. Sowell, Dept. 1110
Sandia Corp.
Albuquerque, New Mexico (1)

79s. L. M. Berry, Organ. 8115
Sandia Corp.
Livermore, California (1)